EGFR/Ras-signaling-dependent CCL20 production in tumor cells critically contributes to angiogenesis and tumor progression

Inaugural-Dissertation

zur

Erlangung des Doktorgrades

der Mathematisch-Naturwissenschaftlichen Fakultät

der Heinrich-Heine-Universität Düsseldorf

vorgelegt von

Anne Schorr, M.Sc.

aus Düsseldorf

Düsseldorf, 2010

Aus der Hautklinik,

Forschungslabor für Dermato-Immunologie und Onkologie

der Heinrich-Heine-Universität Düsseldorf

Gedruckt mit der Genehmigung der

Mathematisch-Naturwissenschaftlichen Fakultät der

Heinrich-Heine-Universität Düsseldorf

Referent: Prof. Dr. Bernhard Homey

Korreferent: Prof. Dr. Dieter Willbold

Tag der mündlichen Prüfung: 18.01.2011

Meinen Eltern

und meinem Freund

Acknowledgment

I would like to express my sincere gratitude to my supervisor Prof. Dr. Bernhard Homey for giving me the opportunity to carry out this interesting research and for the committed guidance. I am also grateful for the financial support and for introducing me already at very early stages to high-caliber scientists in- and outside of the Heinrich-Heine-University research community.

My special thanks are also due to Prof. Dr. Dieter Willbold for co-advising this work.

I am very grateful to Dr. Andreas Hippe who guided me through all steps of this project with patience. He provided me with advice, valuable suggestions and continuous encouragement. Thank you for your help!

I also would like to thank all those who supported me over the years in one way or the other and in particular:

Attila Antal, Virginia Bardeli, Erich Bühnemann, Bettina Alexandra Buhren, Marcel Castrogiovanni, Thomas K. Hoffmann, Anke van Lierop, Sabine Kellermann, Robert Kubitza, Jumana Saleh, Uta and Jochen Schorr

Table of contents

Abbreviations

A

A	absorbance
ADF	Arbeitsgemeinschaft dermatologischer Forschung
AEC	3-amino-9-ethyl-carbazol
AL	Alabama
AR	amphiregulin
AR	Arkansas

B

BAS	bovine serum albumin
B cell	B lymphocyte
BEC	human dermal microvascular blood endothelial cell
bFGF	basic fibroblast growth factor
Bis-Tris	bis(2-hydroxyethyl)amino-tris(hydroxymethyl)methane
BPE	bovine pituitary extract
BSA	bovine serum albumin
BTC	betacellulin

C

C	cysteine
°C	degree Celsius
CA	California
C57BL/6	C57 black 6
CD	cluster of differentiation
cDNA	complementary DNA
CCL	CC-motif chemokine ligand
CCR	CC-motif chemokine receptor
CCX-CKR	chemocentryx chemokine receptor
cm^2	square centimeter
cm^3	cubic centimeter
CO_2	carbon dioxide
CpG	deoxycytidyl-deoxyguanosine
C_T	threshold cycle
CXCL	CXC-motif chemokine ligand
CXCR	CXC-motif chemokine receptor
CX_3CL	CX_3C-motif chemokine ligand
CX_3CR	CX_3C-motif chemokine receptor

D

Δ	delta, difference
3D	three-dimensional
Da	Dalton
DAPI	4',6-diamidino-2-phenylindole
DARC	duffy antigen/chemokine receptor

DC	dendritic cell
DE	Delaware
DEPC	diethylpyrocarbonate
dH_2O	distilled water
DMEM	Dulbecco's modified Eagle's medium
DMSO	dimethyl sulfoxide
DNA	deoxyribonucleic acid
DNAse	deoxyribonuclease
dNTP	deoxyribonucleotide triphosphate
DTT	dithiothreitol

E

EC	endothelial cell
ECL	enhanced chemiluminescence solution
EDTA	ethylenediaminetetraacetic acid
EGF	epidermal growth factor
EGFR	EGF receptor
EGM-2	endothelial cell growth medium-2
18S	18 svedberg
ELISA	enzyme-linked immunosorbent assay
ELR	glutamic acid-leucine-arginine
EPR	epiregulin
ErbB	erythroblastic leukemia viral oncogene
Erk	extracellular-signal regulated kinase
ESDR	European Society for Dermatology Research
ESE-1	epithelium –specific Ets
EST	expressed sequence tags
et al.	et alii, and others
Ets	E-twenty six

F

FACS	flow cytometric analysis
FCS	fetal calf serum
fg	femtogram
Fig.	figure
fpVCT	flat-panel VCT
FSC	forward scatter

G

g	gram
g	gravitational acceleration
GAP	GTPase activating protein
GDP	guanosine-5'-diphosphate
GEF	guanine nucleotide exchange factor
Glu-Leu-Arg	glutamic acid-leucine-arginine
GPCR	G-protein-coupled receptor

G-protein	guanine nucleotide-binding-proteins
Grb2	growth factor receptor-bound protein 2
GST	glutathione-S-transferase
GTP	guanosine-5'-triphosphate

H

h	hour
HaCaT	human adult skin keratinocytes propagated under low Ca2+ and elevated temperature
HB-EGF	heparin-binding EGF
HCl	hydrogen chloride
HER	human epidermal growth factor receptor
HGF	hepatocyte growth factor
HIMEC	human intestinal microvascular endothelial cell
HIV	human immunodeficiency virus
HMEC	human microvascular endothelial cell
HNSCC	head and neck SCC
H_2O	hydrogen oxide, water
H-ras	Harvey-ras
H_2SO_4	sulfuric acid
HRP	horseradish peroxidase
HUVEC	human umbilical vein endothelial cell

I

i.e.	id est, that is
IgG	immunoglobulin G
IGF-1	insulin like growth factor
IL	interleukin

J

JaK	Janus kinases/signal transducers and activators of transcription

K

KC	primary mucosal keratinocytes
kDa	kilo Dalton
K-ras	Kirsten-ras

L

λ	lambda, wavelength
LARC	liver and activation regulated chemokine
LC	langerhans cell
LEC	human lymphatic endothelial cell
L-Glutamate	laevus-glutamate
log	logarithm

M

µ	micro

M	molar
MA	Massachusetts
MALT	mucosa-associated lymphatic tissue
MAPK	mitogen-activated protein kinase
MD	Maryland
MEGM	mammary epithelial cell growth medium
µg	microgram
$MgCl_2$	magnesium chloride
MGM-4	melanocyte growth medium-4
MIP-3a	macrophage inflammatory protein-3a
µl	microliter
µm	micrometer
µM	micromolar
mM	millimolar
MEM	minimal essential medium
min	minute
ml	milliliter
MMP	matrix metalloproteinase
MN	Minnesota
MO	Missouri
mRNA	messenger RNA
MOPS	3-(N-morpholino)propanesulfonic acid

N

n	number
NaCl	sodium chloride
NJ	New Jersey
ng	nanogram
nm	nanometer
nM	nanomolar
NP-40	nonyl phenoxypolyethoxylethanol-40
N-ras	neuroblastoma-ras
NSCLC	non-small cell lung cancer cell
NY	New York

O

OD	optical density
oligo(dt)	oligo(deoxythymidylic acid)

P

P	probability
p90RSK	p90 ribosomal S6 kinase
PDGFB	platelet-derived growth factor B
PDGFBRβ	PDGF receptor β
PE	phycoerythrin
pERK	phosphorylated ERK

pg	picogram
pH	potentia hydrogenii
PI3K/AKT	phosphatidylinositol 3-kinase-AKT
pN	pathologic examination of regional lymph nodes
pT	pathologic examination of primary tumor size
PVDF	polyvinylidene

Q

qRT-PCR	quantitative real-time polymerase chain reaction

R

Raf	rapidly growing fibrosarcoma or rat fibrosarcoma
Ras	rat sarcoma
RasV12	ras with valine at codon position 12
RBD	ras binding domain
RNA	ribonucleic acid
RPMI-1640	Roswell Park Memorial Institute medium
rRNA	ribosomal RNA
RT	room temperature
RTK	receptor tyrosine kinase

S

s	second
SCC	squamous cell carcinoma
SD	standard deviation
SDS	sodium dodecyl sulfate
SDS-PAGE	SDS-polyacrylamide gel electrophoresis
SH2	sarcoma homology 2
SOS	son of sevenless
SSC	side scatter

T

Tab.	table
TAM	tumor associated macrophage
TBS	tris buffered saline
TBST	TBS- Tween® 20
T cell	T lymphocyte
TGF-α	transforming growth factor-α
TNF-α/β	transforming growth factor-α/β
TNM	classification of malignant tumors in tumor size, lymph node involvement and metastasis
Tris	trishydroxymethylaminomethane
Tween® 20	polyoxyethylene (20) sorbitan monolaurate
TX	Texas

U

U	unit

UK	United Kingdom of Great Britain and Northern Ireland
uPA	urokinase plasminogen activators
USA	United States of America
V	
V	volt
VCT	volume computed tomography
VEGF	vascular endothelial growth factor
VEGFR	VEGF receptor
vol.	volume
W	
WI	Wisconsin
X	
XCL	XC-motif chemokine ligand
XCR	XC-motif chemokine receptor

1 Summary

Tumor growth is restricted to a volume of approximately 2-3 mm³ by passive diffusion of nutrients and oxygen. Hence, tumors require the formation of new blood vessels for further growth. The physical process of blood vessel formation from pre-existing microvasculature is referred to as angiogenesis. Chemokines control migratory processes and this superfamily of chemoattractive proteins is among the first protein families to be completely identified at the molecular level. Although their critical role in leukocyte trafficking has recently been identified, little is known about their definite function in tumor-associated angiogenesis.

Here it was demonstrated that the activation of EGFR/Ras regulates chemokine expression. In particular, it was shown that tumors can enhance angiogenesis by upregulating the production of the chemokine CCL20 through the activation of the EGFR/Ras/Raf/MEK/ERK-signaling pathway. Enhanced expression of CCL20 was found to correlate with increased ERK phosphorylation and advanced tumor stage in several types of cancer. Furthermore increased CCL20 expression in tissues of breast cancer patients was associated with poor prognosis of cumulative survival.

Angiogenesis represents a dynamic process involving directional migration of endothelial cells lining all vessels. It was discovered that the CCL20 receptor CCR6 is abundantly expressed on endothelial cells. Activation of CCR6 signaling in endothelial cells induced cell migration and led to enhanced vessel formation. *In vivo*, CCL20 specifically promoted vascularization of Matrigel plugs in wild-type mice, but not in CCR6-deficient mice. Furthermore, tumor growth and vascularization in CCR6-deficient mice were decreased compared to wild-type mice. In conclusion, a novel chemokine-driven mechanism that promotes tumor angiogenesis and cancer progression was identified. These findings not only provide insights into the important role of chemokines in tumor angiogenesis, but also suggest novel targets for anti-cancer therapy.

2 Zusammenfassung

Tumorwachstum ist aufgrund passiver Diffusion von Nährstoffen und Sauerstoff näherungsweise auf ein Volumen von 2-3 mm³ begrenzt. Für ein weiteres Wachstum sind Tumore daher auf die Bildung neuer Blutgefäße angewiesen. Dieser physische Prozess, die Bildung neuer Blutgefäße aus bereits existierenden Mikrogefäßen, wird als Angiogenese bezeichnet. Chemokine sind für ihre Kontrolle migratorischer Prozesse bekannt. Diese Superfamilie chemoattraktiver Proteine gehört zu den ersten, die auf molekularer Ebene vollständig charakterisiert wurden. Obwohl ihre entscheidende Rolle bei der gerichteten Migration von Leukozytenpopulationen schon lange bekannt ist, liegen über ihre genaue Funktion bei der tumorassoziierten Angiogenese nur wenige Erkenntnisse vor.

Im Rahmen dieser Arbeit wurde dargelegt, dass die Expression von Chemokinen durch die Aktivierung von EGFR/Ras reguliert wird. Insbesondere wurde gezeigt, dass Tumore Angiogenese durch die Aktivierung des EGFR/Ras/Raf/MEK/ERK-Signalwegs, und der daraus resultierenden Hochregulierung der Expression des Chemokins CCL20, fördern. Es wurde herausgefunden, dass eine erhöhte CCL20-Expression mit einer erhöhten ERK-Phosphorylierung und einem fortgeschrittenen Tumor-Stadium in verschiedenen Krebsarten korreliert. Des Weiteren war eine erhöhte CCL20-Expression in Tumorgeweben von Brustkrebspatienten mit einer schlechten Prognose des kumulativen Überlebens assoziiert.

Angiogenese ist ein dynamischer Prozess, der die gerichtete Wanderung von Endothelzellen, die alle Gefäße auskleiden, beinhaltet. Hier wurde eine starke Expression des Chemokinrezeptors CCR6, dem spezifischen Rezeptor für CCL20, auf Endothelzellen nachgewiesen. Die Aktivierung des CCR6-Signalwegs in Endothelzellen induzierte deren Migration und förderte die Ausbildung von Mikrogefäßen. *In vivo*, förderte CCL20 spezifisch die Vaskularisierung von Matrigelplugs in Wildtyp-Mäusen, während dieser Effekt in CCR6-defizienten Mäusen ausblieb. Des Weiteren, waren Tumorwachstum und Vaskularisierung in CCR6-defizienten Mäusen im Vergleich zu Wildtyp-Tieren verringert. Im Rahmen dieser Arbeit konnte ein vollkommen neuer chemokin-vermittelter Mechanismus identifiziert werden, der maßgeblich die Tumorangiogenese und Krebsprogression fördert. Diese Ergebnisse verdeutlichen nicht nur die bedeutende Rolle von Chemokinen in der Tumorangiogenese, sie identifizieren neue therapeutische Ziele für die Behandlung von Tumorpatienten.

3 Introduction

Overall, cancer is the second leading cause of death in Germany exceeded only by heart disease. In 2006, more than half a million patients lived with breast cancer, colon carcinoma, head and neck squamous cell carcinoma or melanoma that had been diagnosed 5 years ago[1]. The relative 5-year survival rates of patients suffering from breast cancer are 58% to 76%, for patients with colon carcinoma 53% to 63% and less than every second man diagnosed with head and neck squamous cell carcinoma (HNSCC) survives the first 5 years, and only 50% to 63% of women survive 5-years after diagnosis[1]. The relative 5 year survival rate of 90% for non metastatic melanoma[1] is promising, but the metastatic variant has a very poor prognosis for melanoma patients, because of its insensitivity towards existing therapies, resulting in a median survival rate of 6 months and a 5-year survival rate of less than 5%[2].

In case of melanoma, systemic mono- poly- or immunochemotherapy regimens have achieved only marginal response rates without significant impact on patients' survival. Currently, surgical excision of the primary tumor and the draining regional lymph nodes remains the most effective treatment of patients with nodal disease[3].

Therefore, the most effective strategy to minimize cancer mortality comprises early detection and prevention of disease progression of these cancer types, and innovative therapies against advanced human cancers are urgently needed[4,5,6,7].

Weidner *et al.* demonstrated a direct correlation between the vascular density (number of vessels per high-powered field) and the probability of metastasis in human breast cancer patients[8]. This finding is not limited to breast cancer but has been observed in several other tumors, including carcinoma of the prostate[9,10], lung[11,12], stomach[13], cervix[14], ovary[15], melanoma[16], colon cancer[17,18,19] and in squamous cell carcinoma of the head and neck[20]. Thus, increased vascular density is indicative of increased metastasis and decreased survival for many tumors.

Since tumor progression appears to be angiogenesis dependent and because vascular endothelial cells do not possess the genetic instability that allows cancer cells to develop drug resistance, tumor blood vessels represent an alternative therapeutic target for long-term treatment[21].

Therefore, it is of urgent interest to investigate the molecular mechanisms of angiogenesis-dependent tumor progression.

3.1 The epidermal growth factor receptor (EGFR)

Constitutive activation of the epidermal growth factor receptor (EGFR) and its downstream signaling cascades is a crucial step in the malignant transformation of a wide variety of tumors[22].

The EGF receptor is expressed by nearly all adult human tissues, with exception of hematopoietic cells and regulates cell growth, proliferation and differentiation[23,24]. EGFR belongs to the ErbB family of receptor tyrosine kinases (RTK), which includes four distinct receptors: the EGFR (ErbB-1, HER1), ErbB-2 (Neu, HER2), ErbB-3 (HER3) and ErbB-4 (HER4)[25,26]. EGFR is a 170 kDa transmembrane glycoprotein composed of an extracellular ligand-binding domain, a hydrophobic transmembrane region and an intracellular domain possessing an intrinsic tyrosine kinase function[27]. EGFR is specifically bound and activated by multiple ligands, including epidermal growth factor (EGF), transforming growth factor-α (TGF-α), amphiregulin (AR), heparin-binding EGF (HB-EGF), betacellulin (BTC)[28] and epiregulin (EPR)[29]. There are three major signaling pathways that are activated in response to EGFR activation, comprising of the mitogen-activated protein kinase (MAPK), the phosphatidylinositol3-kinase-AKT (PI-3K/Akt) pathways[27] and the stress-activated protein kinase C and Jak/Stat pathway[26,30].

3.1.1 Signaling by MAPK pathway

The mitogen-activated protein kinase (MAPK) signaling pathway is constitutively activated in many different cell types in presence of extracellular stimuli. This activation results in induction of a multiplicity of cellular responses such as cell differentiation, division, and secretion[31,32,33]. One of the best understood and most important down-stream pathways involved in cancer is the MAPK signaling pathway. Its signaling is initiated by binding of growth factors to the extracellular domain of the growth factor receptor, which leads to a conformational change and to receptor dimerization. Dimerization of the receptors leads to an adjoining of their intracellular tyrosine kinase domains[34]. The juxtaposed kinases are activated by reciprocal transphosphorylation of their tyrosine residues[34] and induce the activation of downstream signaling cascades. The newly created phosphotyrosines are specific binding sites for Src homology 2 (SH2) domains of the downstream effector complex consisting of adapter protein Grb2 and SOS[34], which is a guanine nucleotide exchange factor, and thereby an activator, for the small GTPase Ras[34]. The small G protein Ras is attached to the inner leaflet of the plasma membrane and activates a

signaling cascade of the cytosolic protein kinases Raf, MEK and ERK (Fig. 1)[35]. Phosphorylated ERK (pERK) modulates and phosphorylates many further proteins possessing a variety of regulatory functions. This includes the phosphorylation of other protein kinases (i.e. $p90^{rsk}$), cytoskeletal proteins (such as microtubule-associated proteins), other enzymes (such as cytoplasmic phospholipase A_2), and transcription factors, like members of the ETS transcription factor family[36].

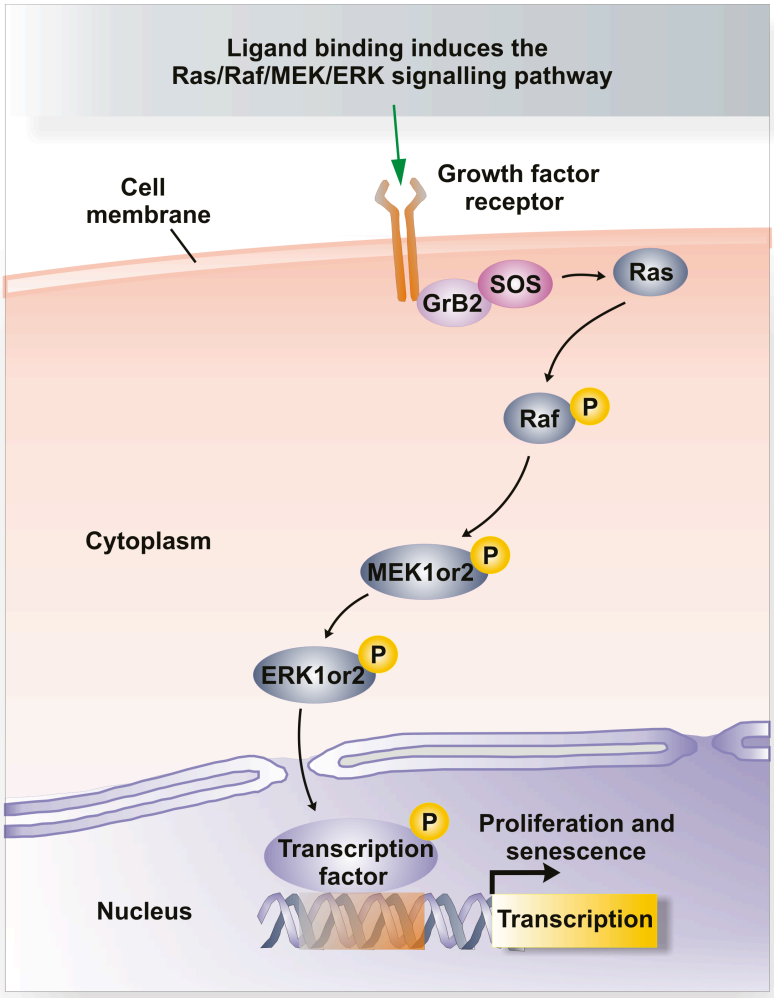

Fig. 1: The Ras/Raf/MEK/ERK mitogen-activated protein kinase (MAPK) signaling pathway.

3.1.2 The proto-oncogene Ras

Alterations in the cellular genome affecting the expression and functions of genes controlling growth and differentiation are considered to be the main cause of cancer[37]. A family of genes that is frequently found to harbor a mutation in human tumors is that of the *ras* genes[37]. This family consists of three functional genes, *Harvey-ras* (*H-ras)*, *Kirsten-ras* (*K-ras*), and *Neuroblastoma*-ras (*N-ras*), which encode highly similar proteins[38]. Point mutations in the three human Ras genes at one of the critical codon positions 12, 13, and 61 result in an altered amino acid at these codons[37]. Like all GTPases, these proteins cycle between an active, guanosine triphosphate (GTP)-bound form, and an inactive guanosine diphospate (GDP)-bound form[39]. Two families of proteins, guanine nucleotide exchange factors (GEFs) and GTPase activating proteins (GAPs), activate and inactivate the GTPases[39]. Ras-GTP sustains an activating signal for some time, as its intrinsic rate of GTP hydrolysis is very low (0.005 s^{-1})[34]. Point mutations (such as substitution of valine for glycine-12 (RasV12)) can constitutively activate Ras by reducing its GTPase activity[34] leading to a constitutively activated MAPK signaling pathway and an altered gene expression profile.

Altogether, abnormal activation or expression of these signaling proteins has been associated with cancer. In detail, overexpression of the EGFR tyrosine kinase gene (*c-erb* B-1)[40], point mutations of the *ras* oncogenes[37,41,42], resulting in constitutively activated Ras proteins[34], or constitutive activation of ERK[22,40] were found in several human cancers.

Recently it could be observed, that the EGFR system is involved in the expression of angiogenic factors[43]. For example, treatment of human glioma cells with the endothelial growth factor (EGF) led to the expression of the vascular endothelial growth factor (VEGF)[44]. Analogously, treatment of prostate cancers cells, which were cultured *in vitro* or injected in the flank of nude mice, with the tyrosine kinase inhibitor gefitinib, resulted in decreased expression of both VEGF and the basic fibroblast growth factor (bFGF)[45]. Donation of the EGFR tyrosine kinase inhibitor PKI 166 to nude mice with implants of pancreatic carcinoma cells, induced a significant reduction of tumor derived VEGF and vascular density[46,47]. These findings suggest a pivotal role of EGF receptor signaling in tumor-associated angiogenesis.

3.2 Angiogenesis

With induction of the cellular hyperproliferation during tumor development, tumor outgrowth is usually restricted to a volume of no more than 2-3 mm^3 [48]. This phase, in which the tumor obtains oxygen and nutrients by diffusion from adjacent vessels, is often called the avascular phase. During this stage tumor-associated formation of new blood vessels is not observed[48]. Avascular tumors can keep a steady state, where proliferation of tumor cells and apoptosis are in balance and net increase in tumor volume does not appear[48]. To pass the size limit, tumors must gain access to an increased supply of oxygen and nutrients and have to obtain the possibility to dispose metabolites of toxicological concern[48]. These increasing needs of growing tumors mostly implicate angiogenesis[48].

3.2.1 What is angiogenesis?

The proceeding growth, expansion and remodeling of existing vessels into a mature vascular network is referred to as 'angiogenesis'[49]. This process is characterized by a combination of new vessels sprouting from the sides and ends of pre-existing ones (sprouting angiogenesis), or by longitudinal division of existing vessels with periendothelial cells (intussusception)[49]. Angiogenesis is largely restricted to embryogenesis and is rare in adults[39]. It has been reported to play an important role in both health and disease[50,51,52]. Indeed, under nomal physiological conditions, the vasculature is remarkably quiescent, with angiogenesis occuring mainly during physiological menstruation and pathological wound healing[39]. Nonetheless, many pathologies are characterized by their induction of vessel growth from pre-existing vasculature including atherosclerosis, endometriosis, osteomyelitis, diabetic retinopathy, rheumatoid arthritis, psoriasis, and tumor growth[39].

3.2.2 Morphology of vessels

In general, the wall of vessels is composed of three layers, the *tunica intima* (innermost layer), the *tunica media* (middle layer) and the *tunica externa* (outermost layer)[53]. The *tunica intima* is lined by a single layer of specialized cells called endothelial cells (ECs)[39,53]. ECs play an important role in angiogenesis as they express a wide variety of receptors, like growth factor or cytokine receptors, enabling ECs to respond to numerous different angiogenic and angiostatic factors[54,55,56,57,58]. The entire number of ECs of the human body amounts to $(1–6)\times10^{13}$ forming an organ weighting almost 1 kilogramm[59]. In case of blood endothelial cells, they uniquely (together with platelets) exhibit 0.1 µm wide

and 3 µm long membrane-bound Weibel-Palade bodies, which are storage organelles containing the von Willebrand factor[59]. This factor is mainly involved in hemostasis by connecting platelets to collagen of the vessel´s wall[60]. The *tunica intima* is completed by a basement membrane and surrounded by a dispersive layer of pericytes embedded within the EC basement membrane[61]. The *tunica media* is comprised of smooth muscle cells. The vessels' outermost layer is the *tunica externa*, also known as *tunica adventitia* encompassing the *tunica media*. The adventitia consists of connective tissue components like fibroblasts, together with matrix and elastic laminae[61].

Formation of vessels is initiated by the arrangement of ECs in so called tubes (Fig. 2A). These tubes represent nascent vessels, maturing into the specialized structures of capillaries (Fig 2B), arterioles (small arteries), venules (small veins) (Fig. 2C), arteries, veins (Fig. 2D) or lymphatic vessels (Fig. 2E).

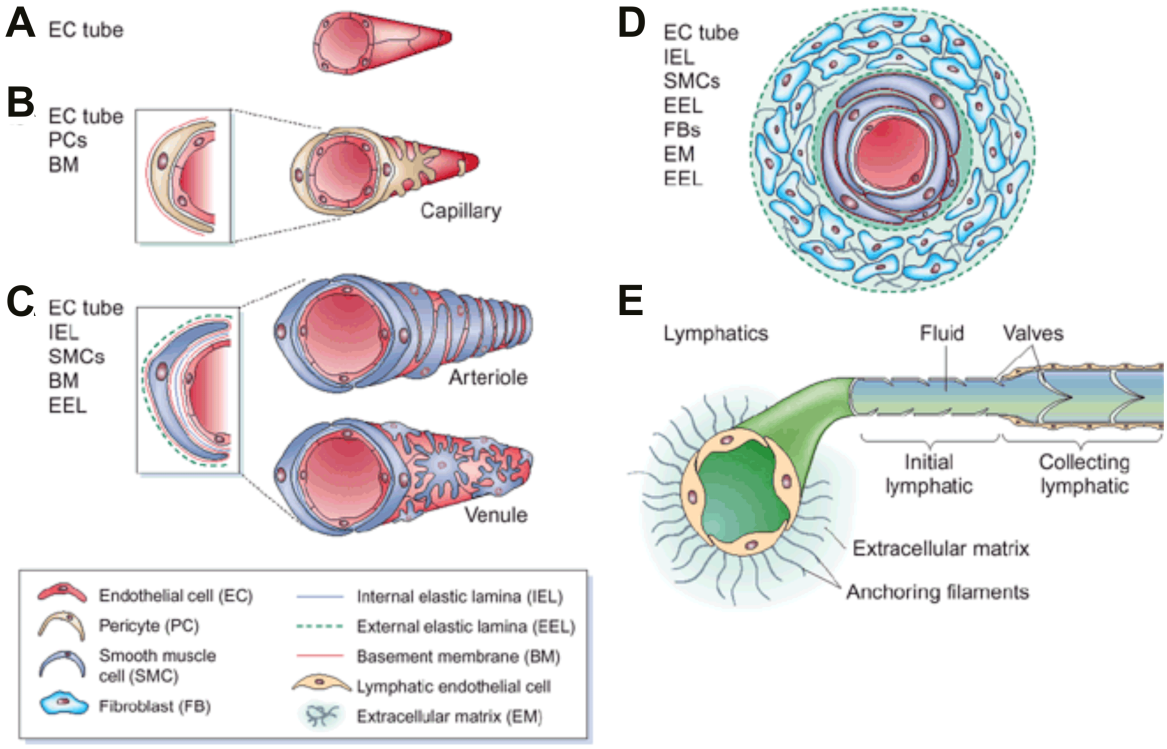

Fig. 2: Schematic composition of nascent and mature vessels. (**A**) Nascent tube consisting of endothelial cells; (**B**) Capillaries; (**C**) Arterioles and venules; (**D**) Larger vessels (arteries and veins); (**E**) Lymphatic capillary; Adapted and modified from[61].

3.2.3 Molecular mechanisms of angiogenesis

The establishment of new blood vessels from preexisting vasculature includes several steps. This requires the degradation of the basement membrane surrounding the blood vessel and the break down of cell-cell contacts between endothelial cells followed by the migration of endothelial cells in direction of an angiogenic stimulus. Finally, proliferation of these cells results in the formation of vessel lumen and a new vascular system[62,63].

After degradation of the basement membrane by urokinase plasminogen activators (uPA) or matrix metalloproteinases (MMPs)[39] endothelial cells migrate into the adjacent tissue by means of chemotaxis[39]. Chemotaxis is the oriented movement of cells in response to the concentration gradient of chemical substances in their environment. In the last years, many factors that fuction as angiogenic regulators came into focus[39], like fibroblast growth factors (FGFa and FGFb), transforming growth factors (TGFα and TGFβ), hepatocyte growth factor (HGF), tumor necrosis factor (TNFα), angiogenin, interleukin-8, angiopoetins and chemokines[64]. However not all of these molecules specificly bind to endothelial cells, and only some of them have direct effects on endothelial cells in culture[64]. The most established and investigated might be the vascular endothelial growth factor A (VEGF-A). Its angiogenic activity results in the development of a specialized endothelial cell, termed tip cell[39], which develops filopodia extending in direction of the angiogenic stimulus[65] by interaction with the corresponding receptor VEGFR2[65]. Inactivation of the *VEGFR2* gene in mice results in embryonic lethality, with lack of development of both hematopoietic and endothelial lineages, supporting the critical importance of this receptor at that developmental stage[49]. Behind these tip cells, other endothelial cells begin to proliferate, elongating the developing, tubelike structures[39].

Following endothelial cell chemotaxis, vessels mature and are stabilized by the recruitment of mural cells by expressing the homodimer platelet-derived growth factor B (PDGFB). PDGFB is mainly expressed by endothelial tip cells, generating a concentration gradient to attract PDGFRβ receptor-expressing pericytes to sites of newly formed nascent tubes to form the new vessel's wall[66,67]. In mice deficient in expression of this growth factor, defects in the capillary wall formation due to insufficient content of pericytes were found[68].

3.2.4 The angiogenic switch

The regulation of angiogenesis is dependent on the balance of angiogenic and angiostatic factors present in the microenvironment[69]. Under homeostatic conditions, turnover of endothelial cells forming the inner lining of vasculature is measured in months or years[70,71,72]. However, under conditions requiring rapid neo-vascularization such as wound healing or tumor angiogenesis, the balance between angiogenic and angiostatic factors in the microenvironment is rapidly shifted in favor of angiogenic factors. This transition from the homeostatic to the angiogenic phase is referred to as the "angiogenic switch"[48] enabling the development of new vessels efficiently within days[69,72].

The molecular mechanism of angiogenesis remains elusive and requires a complex interaction of a wide set of further angiogenic and angiostatic factors. In the last 20 years, many factors that have angiogenic activity have been identified[39]. One of those factors are small cytokine-like proteins called chemokines.

3.3 Chemokines

Chemokines are a family of small (8-14 kDa) cytokine-like, mostly basic, structurally related chemotactic molecules. They are known to regulate leukocyte trafficking and have been found to play an important role in the regulation of tumor cell migration to sites of organ-specific metastases[73]. Chemokines signal through interactions with G-protein-coupled receptors composed of seven transmembrane- spanning domains[74]. They represent the first protein superfamily completely characterized at the molecular level. About 22 years ago the first chemokine, now called CXC chemokine ligand 8 (CXCL8), but previously known as interleukin 8 (IL-8), was described as a neutrophil-activating factor[75]. The most widely studied chemokine receptors might be CCR5 and CXCR4, which mediate T lymphocytes recruitment to secondary lymphoid organs and sites of inflammation[76], but also serve as coreceptors for HIV in the infection of these $CD4^+$ T cells[75].

3.3.1 The chemokine superfamily

To date, there are 46 chemokines and 18 functionally active chemokine receptors identified in humans[74,77]. Chemokines can be classified into four subclasses based on the position of the first two cysteine residues in their amino acid sequence[78]. The first group of chemokines, called the CC subfamily (thus named because of the juxtaposed first two cysteine residues), includes 26 members, whereas the CXC subfamily (which comprises a single variable amino acid between the first two cysteins) is composed of 17 members[79]. Two smaller subclasses are represented by the CX3C family (one member) (three amino acids between the first two cysteines) and the XC family (two members), which is devoid of the first and third cysteines[79]. Biological effects of chemokines are mediated by binding to chemokine receptors, which are a subfamily of class A (rhodopsin-like) g-protein-coupled receptors (GPCRs)[79]. There are 10 CCR family members and 7 CXCR family members in addition to XCR1 and CX3CR1 (Fig. 3)[79]. Furthermore, there are aberrant receptors, which decoy ligands with high affinity but do not elicit signal transduction after binding to the ligand[79]. These receptors include D6, DARC and CCX-CKR (Chemocentryx, chemokine receptor).

Chemokines can alternatively be devided into two groups depending on their chromosomal gene locations[78]. The first group comprises chemokine genes located in large clusters at particular chromosomal locations. Chemokines encoded by these gene

clusters are characterized by a complex and promiscuous ligand-receptor relationship and bind to multiple receptors[78] (Fig. 3), suggesting the possibility of functional redundancy. Although many chemokines and chemokine receptors are unspecific in their interactions, a minority of chemokines binds specific to their receptors[79]. These chemokines are CCL20 and CCL25, CXCL13 and 16, as also CX3CL1 (Fig. 3). These non-cluster chemokines are known to be relatively conserved between different species and show a tendency not to act on multiple receptors[78]. In particular, CCL20 is the sole chemokine ligand of its receptor, CC chemokine receptor-6 (CCR6)[80,81].

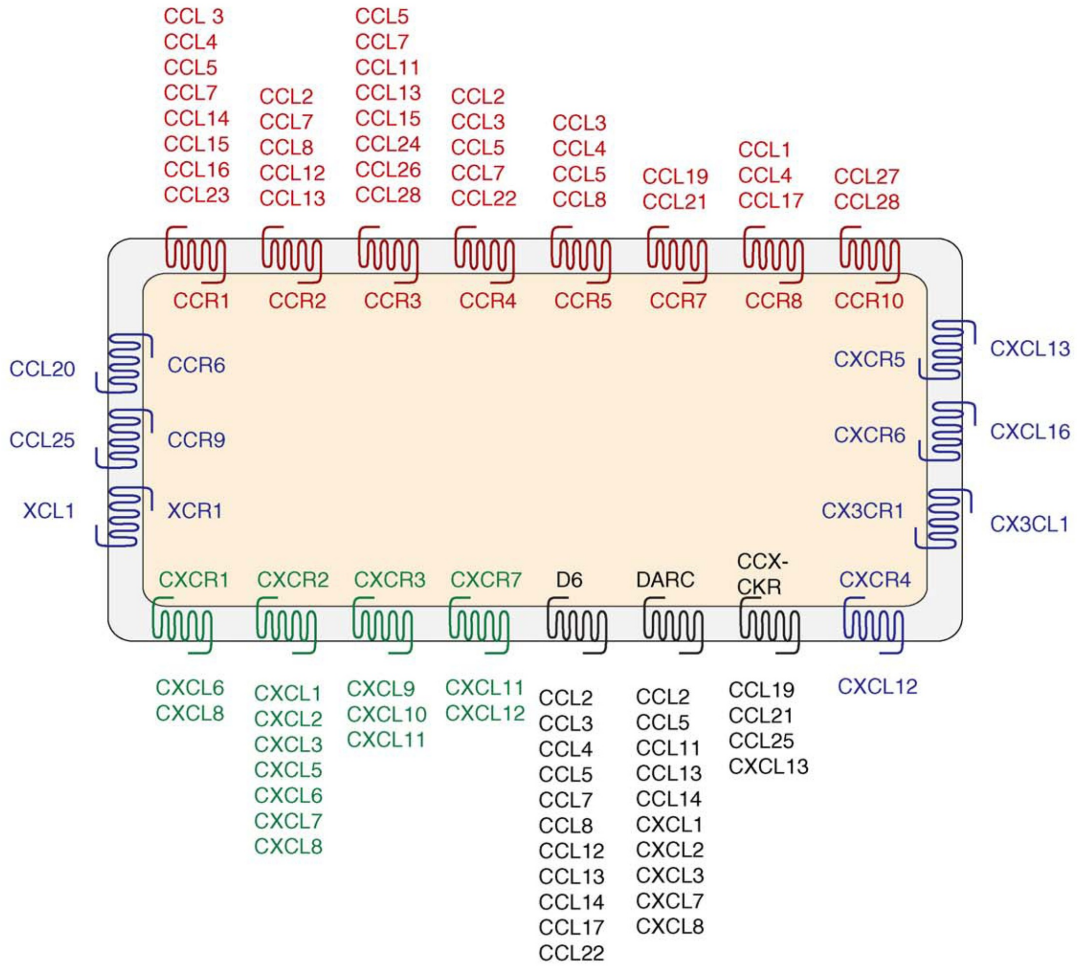

Fig. 3: Chemokines and their receptors. A single receptor can interact with multiple chemokines, and most chemokines can interact with multiple receptors. This is the case for most CC (red) and CXC (green) chemokines. Decoy, not signaling, receptors (black) can also be bound by multiple chemokines. In contrast, a minority of receptors (blue) are specific for only one ligand[79]; Adapted from[79].

3.3.2 Angiogenic chemokines

Due to their ability to induce both, proliferation and migration, chemokines and their receptors represent ideal candidates for proliferative and chemotactic responses of endothelial cells during angiogenesis.

Among the four chemokine subfamilies, CXC chemokines have been demonstrated to play an extensive role in angiogenesis[82]. The CXC chemokines can be further subdivided based on the presence or absence of a three-amino-acid motif (Glu-Leu-Arg) present at the NH_2-terminus, namely the ELR-motif[83]. ELR^+ CXC chemokines (CXCL1, CXCL2, CXCL3, CXCL5, CXCL6, CXCL7, and CXCL8) are angiogenic factors, whereas ELR^- members (except CXCL12) function as angiostatic factors to inhibit growth and formation of blood vessels[79]. All angiogenic ELR^+ CXC chemokines signal by binding to and activation of their receptor CXCR2[84]. CXCR2 was shown to be expressed in human microvascular endothelial cells (HMEC) at the protein level by both western blot analysis and immunohistochemistry[84]. Additionally, this receptor could be detected on mRNA level in human umbilical vein endothelial cells (HUVECs)[85], HUVECS also express the receptor CXCR1[85]. The chemokine receptor CXCR1 was supposed to mediate angiogenic responses because of its potency to be activated by binding of CXCL6 and CXCL8[78]. For instance, primary cultures of human intestinal microvascular endothelial cells (HIMEC), expressing CXCR2, but not CXCR1, responded to CXCL8 with rapid stress fiber assembly, enhanced proliferation, and chemotaxis[86].

The CC family of chemokines has also been implicated in angiogenic progression and development[82]. For instance, when implanted into rabbit cornea, CCL2 was potently angiogenic similar to VEGF-A, the specific angiogenic vascular endothelial growt factor[87]. But CCL2 also enhanced accumulation of macrophages[87] suggesting indirect effects by recruited macrophages. In addition to CCL2, other members of the CC subfamily of chemokines have been shown to be implicated in angiogenesis. CCL1, CCL11, CCL15, CCL16 and CCL23 have all been demonstrated to induce endothelial cell migration *in vitro* and mediate angiogenesis *in vivo*[82]. Furthermore, CCL5 and CCL23 have been shown to up-regulate the MMP9 and MMP2, respectively, implicating their activity in angiogenesis[88,89].

3.3.3 Chemokines in tumor-associated angiogenesis

During the avascular phase that precedes angiogenesis, tumor growth is limited by the rate at which nutrients and oxygen diffuse across the outer tumor boundary [90]. Chemokines have been shown to participate in angiogenesis and tumor progression under homeostatic and neo-plastic conditions[69].

Especially, the ELR^+ CXC chemokines came into focus and became generally known to be important mediators of tumor associated angiogenesis in many different tumor types. For instance, CXCL1, CXCL2 and CXCL3 are highly expessed in human melanoma[91]. When human *CXCL1, CXCL2* and *CXCL3* genes were transfected into immortalised murine melanocytes, which naturally do not generate tumors, cells were able to form tumors in immuno-incompetent mice[91,92]. Depletion of CXCL1, CXCL2 and CXCL3 in tumors resulted in a significant reduction of tumor-derived angiogenesis, which directly correlated with inhibiton of tumor growth[91,92].

Apart from CXC chemokines, CC chemokines are also known to be implicated in angiogenesis-driven tumorigenesis. For instance, CCL2 is abundantly expressed by estrogen receptor negative breast cancer cells[93] and its gene expression is reported to be upregulated in colon cancer[82]. Furthermore tumor-associated macrophages (TAM) in the tumor stroma exhibit increased expression of CCL2 and TAM agglomeration correlates with poor prognosis and recurrence of disease[94,95]. Its receptor CCR2 is expressed on HUVECS and aortic endothelial cells[54]. This suggests the involvment of CCL2 in tumor-associated angiogenesis.

Altogether, chemokines appear to play an important role in the regulation of angiogenesis associated with tumorigenesis relevant to cancer.

3.3.4 Angiostatic chemokines

Angiostasis is the inhibition of the outgrowth of new blood vessels from pre-existing vasculature. This restraint is the normal state (homeostasis) of vessels in human adults[96,97]. The ELR^- CXC chemokines CXCL4, CXCL9, CXCL10, CXCL11 and CXCL14 are reported to be angiostatic[83,98,99,100,101]. With exception of CXCL14, whose receptor is still unknown, all angiostatic chemokines bind to the chemokine receptor CXCR3. Two alternative splicing variants of this receptor were found namely CXCR3-A and CXCR3-B[102]. CXCR3-B and not CXCR3-A was expressed by primary human microvascular endothelial cells (HMEC) and treatment of these cells with CXCL4, CXCL9, CXCL10 and

CXCL11 resulted in inhibition of proliferation, viability and growth[102]. Furthermore, monoclonal antibodies generated by immunized BALB/c mice were used to specifically recognize CXCR3-B reacting with endothelial cells from neoplastic (abnormal proliferative) tissues, providing conclusion that CXCR3-B is also expressed *in vivo* and may determine the angiostatic capacity of CXC chemokines[102]. Relating to CXCL14, Shellenberger *et al.* observed that CXCL14 inhibited microvascular endothelial cell chemotaxis *in vitro* and additionally inhibited angiogenesis *in vivo* in a rat corneal micropocket assay[100]. These findings suggest the involvement of the still unknown putative CXCL14 receptor in angiostasis.

3.4 Aim of the thesis

Recent findings suggest that EGFR-signaling regulates chemokine production within the tumor microenvironment. Sparmann and co-workers have demonstrated that activation of the Ras proto-oncogene in cancer cells results in the up regulation of CXCL8, which in turn promotes angiogenesis and tumor growth[103]. In a recent study, our group could demonstrate that human keratinocyte-derived skin tumors may evade T cell-mediated antitumor immune responses by down regulating the expression of CCL27 through the activation of epidermal growth factor receptor (EGFR)-Ras-MAPK-signaling pathways[104]. Furthermore, activation of the EGFR by EGF increases CXCR4 expression and the migratory capacity of non-small cell lung cancer cells (NSCLC)[105]. Collectively, these results hint at a role for EGFR activation in chemokine-mediated (lymph)angiogenesis, invasion, metastasis and immune escape of tumors.

The questions that need to be addressed are:

- Are there further chemokines regulated by the MAPK signaling pathway?
- From regulatory to expressional level: Do tumors express EGFR/Ras-regulated CCL20 and what are the physiological and clinical effects of tumor-derived CCL20 expression?
- Pro- versus anti-tumor effects: A novel role for CCL20 in tumor biology?

4 Materials and Methods

4.1 Buffers and solutions

Table 1: List of different buffers and solutions. Chemicals were acquired from Sigma- Aldrich, Saint Louis, MO, USA.

EDTA	0.5 M EDTA	adjust to pH 8.0
1x Lysis/Binding/Wash Buffer	25 mM Tris/HCl	pH 7.5
	150 mM NaCl	
	5 mM $MgCl_2$	
	1% NP-40	
	5% Glycerol	
MOPS buffer	0.4 M MOPS	
	0.17 M Sodium Acetate	
	0.01 M EDTA	adjust to pH 7
2x Reducing Sample Buffer	1 part β-mercaptoethanol	
	20 parts 2x SDS Sample Buffer	
2x SDS Sample Buffer	25 mM Tris/HCl	pH 6.8
	2% Glycerol	
	4% SDS (w/v)	
	0.05% Bromophenol blue	

Transfer buffer	27 mM Glycine 48 mM Tris-base 0.037% SDS 20% methanol	
Tris Buffered Saline (TBS)	25 mM Tris/HCl 150 mM NaCl	pH 7.5
Tris Buffered Saline, Tween-20 (TBST)	0.05% Tween-20 in TBS	

4.2 Biopsy samples

Six-millimeter punch biopsies were taken after obtaining informed patient's consent. Biopsies were acquired from breast cancer patients, head and neck squamous cell carcinoma and melanoma patients. Normal skin and normal breast samples were obtained from individuals undergoing plastic surgery. Tumor tissue microarrays of breast cancer and head and neck squamous cell carcinoma were acquired from Pantomics, Inc. (San Francisco, CA, USA), Super Bio Chips (Seoul, Korea) and US Biomax, Inc. (Rockville, MD, USA). Colon carcinoma tumor tissue microarrays were provided by N. Stoecklein (Department of General-, Visceral- and Pediatric Surgery, University Hospital Düsseldorf, Germany).

4.3 Mice

Wild-type-C57BL/6-mice were provided by Taconic, Denmark. C57BL/6-CCR6$^{-/-}$-mice[106] were a kind gift from S. A. Lira (Immunobiology Center, Mount Sinai School of Medicine, New York, NY, USA) and housed in the animal facility of the Heinrich-Heine-University

Düsseldorf, Germany. Experiments were approved by the animal ethics committee of the Bezirksregierung Düsseldorf.

4.4 Cell culture

Human primary epidermal keratinocytes were purchased from Cambrex (East Rutherford, NJ, USA) and were grown in keratinocyte medium (Gibco, Invitrogen, Carlsbad, CA, USA) supplemented with recombinant EGF (0.1-0.2 ng/ml), bovine pituitary extract (BPE) (20-30 µg/ml) and L-Glutamate (2 mM) (PAA, Pasching, Austria). Cells were treated with 500 nM or 1,000 nM erlotinib (Roche, Mannheim, Germany) or left untreated. Erlotinib stock solution (10 mM) (Roche) was prepared by dissolving erlotinib powder in DMSO (Sigma-Aldrich). The treatment solutions were freshly diluted to used concentrations in cell specific medium. Usually, cells were treated for 24 h. Primary human keratinocytes had been transfected with an activating mutant of Ras (H-RasV12) in the expression vector pDCR (a gift from Craig Webb, Frederick, MD) as described by Tscharntke *et al.*[107]. HaCaT keratinocytes and H-RasV12-transfected HaCaT clones were cultured as described previously[108]. The following human breast cancer and melanoma cell lines were obtained from the ATCC and cultured as recommended by the provider: DU-4475, MCF-7, T-47D, Hs578T, MDA-MB-468, MDA-MB-361, MDA-MB-435P, MDA-MB-435S, MeWo, SK-Mel-2, SK-Mel-28, SK-Mel-31, HT-144, Malme-3M and B16F10. MV3 and BLM melanoma cells were a gift from D. J. Ruiter (Department of Pathology, University Medical Center Nijmegen, The Netherlands). Cells were cultured in DMEM (Lonza, Basel, Switzerland) supplemented with 10% fetal calf serum (FCS) (Biochrom AG, Berlin, Germany). TXM-14 and TXM-30 cells were obtained from I. J. Fidler (Department of Cancer Biology, Cancer Metastasis Research Center, Houston, TX, USA) and cultured as described[109]; UKRV-Mel-4 and UKRV-Mel-30 melanoma cells were a gift from D. Schadendorf (Department of Dermatology, Venereology and Allergology, University Medical Center and Medical Faculty Mannheim, University of Heidelberg, Mannheim, Germany) and cell lines were grown in RPMI-1640 medium (Lonza) supplemented with 10% FCS (Biochrom AG). UD-SCC cell lines were derived from primary tumors of the head and neck region and UM-SCC cell lines were generated from lymph node metastases by the Institute of Otorhinolaryngology of the University Hospital Düsseldorf, Germany and cultured in DMEM (Lonza) with 10% FCS (Biochrom AG) (UD-SCC 1-2, 4, 7-8, UM-SCC 10B, 17B, 24A, 24B) or in MEM (Gibco) with 10% FCS and 2% L-Glutamine

(PAA) (UD-SCC 3, 6, UM-SCC 10A, 17A). Human primary mammary epithelial and human primary melanocytes were obtained from Clonetics (San Diego, CA, USA) and cultivated in MEGM complete medium and MGM-4 medium (all Lonza). Human primary mucosal keratinocytes were generated from punch biopsies and cultured similarly to the primary human keratinocytes. Human dermal microvascular blood endothelial cells (BEC) and human lymphatic endothelial cells (LEC) were cultured in endothelial cell growth medium (EGM-2) and purchased from Lonza. All cells were routinely cultured in an incubator at 37°C with 95% humidity and 5% CO_2 (INCO 2, Memmert, Schwabach, Germany) and all media were supplemented with 1% of a mixture of antibiotics (penicillin 100 U/ml, streptomycin 100 µg/ml) (PAA).

4.5 Total RNA isolation

RNA extraction was realized from cells by using the TRIzol® Reagent, a cell lysing monophasic solution of phenol and guanidine isothiocyanate. Addition of chloroform separates the organic and aqueous (containing RNA) phases. Phenol removes the proteins from nucleic acid samples during isolation.

Briefly, to lyse cells 1 ml of TRIzol® Reagent (Invitrogen, Carlsbad, CA) was added to 1 well of a 6-well plate. After adding $^1/_5$ volume chloroform (Merck, Darmstadt, Germany), cells were vortexed and subsequently centrifuged (15 min, 12,000 g, 4°C) (Biofuge 13R, Heraeus Sepatech GmbH, Osterode, Germany). Following centrifugation, the aqueous upper phase was transferred into a new tube and RNA precipitation was achieved by adding ½ volume isopropanol (Merck). The solution was mixed by vortexing, incubated overnight at -20°C, and finally centrifuged (16.100 g, 30 min, 4°C) (Centrifuge 5415R, Eppendorf, Wesseling-Bezdorf, Germany). The RNA precipitate was visible as a pellet on the bottom and on the side of the tube. To remove any residual salt the pellet was washed in 1 ml of 80% ethanol (Merck) after supernatant had been carefully removed. Again the sample was centrifuged for (16.100 g, 30 min, 4°C) (Centrifuge 5415R, Eppendorf). After removal of supernatant, the pellet was dried for 10 min at room temperature (RT) and subsequently dissolved in an appropriate volume (usually 50 µl) of DEPC-treated H_2O (Roth, Karlsruhe, Germany). Samples were stored at -80°C.

4.6 OD measurement

RNA yield was determined using NanoDrop™ 2000 (Thermo Scientific, Wilmington, DE, USA) photometer. RNA concentration was measured according to the manufacturer's manual. The optical density (OD) was measured at 260 nm (relative absorbance maximum of RNA) and 280 nm (relative absorbance maximum of aromatic residues of proteins). An A_{260}/A_{280} absorbance ratio between 1.8 to 2.1 indicated that extracted RNA was devoid of any appreciable protein, salt, or solvent contamination.

4.7 Complementary DNA (cDNA) synthesis

cDNA was synthesized from different messenger RNA (mRNA) templates using reverse transcriptase enzyme Superscript II (Invitrogen).

Since DNA removal is necessary for subsequent applications, DNase digestion was performed. Therefore, 4 µg of total RNA was mixed with 40 U RNasin (Promega, Madison, WI, USA), 10 U recombinant DNase I (Roche) and 5 x first strand buffer (Invitrogen). RNase-free water was added to a final volume of 16 µl and prepared mixes were incubated for 20 min at 37°C, 10 min at 70°C, and thereafter placed at 4°C.

RNA was primed with a mixture of 1 µg of anchored oligo$(dt)_{12-18}$ (Invitrogen) and 0.2 µg of random hexamer primers (Promega). RNase-free water was added to a final volume of 20 µl and samples were incubated for 10 min at 70°C in order to reduce RNA secondary structures.

Then, 40 U RNasin (Roche), 3.57 mM DTT (Invitrogen) and 1.61 mM dNTP mix (Bioline USA Inc., Tauton, MA, USA) were added in 5 x first strand buffer (Invitrogen) to a final sample volume of 28 µl.

The reaction was gently mixed and after an initial incubation step of 2 min at 42°C for optimal primer annealing, cDNA synthesis was carried out after addition of 400 U Superscript II (Invitrogen) resulting in a final volume of 30 µl. Samples were incubated for 50 min at 50°C followed by an incubation step of 10 min at 70°C to inactivate the enzyme (Trio-Thermoblock, Biometra, Göttingen, Germany). Thereafter, samples were stored at -80°C.

4.8 Quantitative real-time PCR (qRT-PCR) analysis

In order to quantitate differences in mRNA expression qRT-PCR was performed. During 40 cycles of qRT-PCR a specific sequence of the gene was amplified in presence of the fluorescent dye SYBR® Green. This dye binds with high affinity to double stranded DNAs. The resulting DNA-dye-complex emits green light (λ_{max} = 522 nm) detected with the Applied Biosystem 7000 System (Applied Biosystems Inc., Foster City, CA, USA) after each cycle (real time). The more abundant the amplification product, the higher the fluorescence emission. Reaching a fluorescence threshold, the current cycle is called C_t-value (threshold cycle) and used for further analysis. Genes expressed at higher rates have higher starting copy numbers and, therefore, appear earlier during the amplification resulting in lower C_t-values. As an internal standard gene expression analysis of 18S rRNA was used since it is expressed at relatively constant levels throughout different cells. The 18S rRNA Taqman qRT-PCR system relies on the 5' to 3' exonuclease activity of the Taq man polymerase, which is able to cleave phosphodiester bonds of nucleotide sequences. In Taq man assays a short nucleotide sequence called probe is linked with a fluorescent dye at the 5' end (VIC™) and a quencher dye at the 3' end (TAMRA™). During the annealing stage of the PCR both, primers and probe (in between the primers), anneal to the target gene. When the Taq polymerase reaches the probe its 5' to 3' exonuclease degrades the probe and thereby separates the fluorescent dye from the quencher dye resulting in an increase of fluorescence which can be detected by the Applied Biosystem 7000 System (Applied Biosystems).

For a final reaction volume of 25 µl per well, the following gene specific mixes were prepared:

	Primer forward	**Primer reverse**	**Target Probe**	**Detection Mix**	**cDNA**
CCL20 (SYBR® Green)	200 nM	200 nM		½ vol.	2.5 ng/µl
Eukaryotic 18S rRNA (TaqMan®)	60 nM	60 nM	60 nM	½ vol.	2.5 ng/µl

The following PCR program was applied:

temperature	time	
50°C	2 min	
95°C	10 min	
95°C	15 s	40 cycles
60°C	1 min	

In order to prove, whether primer-dimer artifacts had affected the reaction (in case of SYBR® Green detection) a dissociation protocol was always carried out after termination of the PCR program. In this protocol, the temperature is gradually increased to melt the products formed during the PCR reaction. The melting point can be easily detected since the fluorescent signal decreases as DNA double strands separate and therefore intercalated SYBR® Green is released. Different PCR products obtained with the same primer pair should have approximately the same melting point.

For absolute quantification, standard curves were prepared from 0.01 pg/µl DNA to 1,000 pg/µl DNA. Quantity of gene expression was calculated automatically by the Applied Biosystem 7000 System (Applied Biosystems, Inc.):

Quantity [pg] = m x + b

Where m is the slope and b is the Y-axis intercept of the standard curve line. The x is the C_t-value obtained for specific gene in a specific sample.

Quantity was standardized to the gene expression of 18S rRNA:

$$Quantity_{standardized}\ [fg] = Quantity\ [pg] \cdot 2^{(Ct18SrRNA - \underline{Ct}18SrRNA)} \cdot 10^3$$

Where $\underline{C_t}$18SrRNA is the mean of all C_t-values obtained for the 18S rRNA of all samples.

Gene expression was illustrated as mean values ± standard deviation.

4.9 Ras activity assay

The activation of H-Ras of *H-RAS* transfected keratinocyte HaCaT cells was analyzed by using the Active Ras Pull-Down and Detection Kit as described by the manufacturer (ThermoFisher Scientific Pierce Protein Research Products, Waltham, MA, USA). Ras is active when bound to GTP and inactive when bound to GDP. Active Ras binds specifically to Ras-binding domain (RBD) of Raf1, leading to its activation. The kit provides a Glutathione-S-transferase (GST) -fusion protein of the Ras-binding domain of Raf1. GST binds with high affinity to glutathione. Therefore, the RBD of Raf1 can be used as a probe to specifically isolate the active form of Ras.

4.9.1 Lysis of cells

Adherent cells were grown to 80-90% confluency. Culture medium was removed and cells were rinsed with ice-cold TBS. 1 ml Lysis Buffer was added per 75 cm² tissue culture flask (Cellstar® greiner bio-one, Frickenhausen, Germany) and cells were scraped and transferred to a microcentrifuge tube (safe-lock-tube 1.5 ml, Eppendorf, Hamburg, Germany). After a 5 min incubation step on ice, cells were centrifuged (Centrifuge 5415 R, Eppendorf) at 16,000 g at 4°C for 15 min. The supernatant was transferred to a new tube.

4.9.2 Protein measurement

Protein concentration was determined according to Bradford. For each sample Bradford protein reagent (Bio-Rad Laboratories Inc., Hercules, CA, USA) was diluted 1:4 in water

(dH_2O) without (control) and with protein lysate added to a volume of 1 ml. The optical density (OD) was determined at 595 nm (Ultrospec 3000, Pharmacia Biotech, GE Healthcare, Buckinghamshire, UK). Absolute quantification was carried out with an appropriate standard curve of bovine serum albumin (BSA) (Sigma-Aldrich).

4.9.3 Affinity precipitation of activated Ras

Spin cups were placed into collection tubes and mounted with 100 µl of the 50% resin slurry, centrifuged at 6,000 g for 30 seconds and washed with 400 µl Lysis Buffer. GST-Raf1-RBD was thawed on ice and immediately 80 µg (33 µl) GST-Raf1-RBD and 700 µl of the cell lysate (containing at least 500 µg of total proteins) were transferred to the spin cup and vortexed. After 1 hour of incubation on ice, cups were centrifuged at 6,000 g for 30 seconds and transferred into a new collection tube. The glutathione agarose resin was washed three times by addition of 400 µl Lysis/Wash Buffer and by centrifugation at 6,000 g for 30 seconds. Spin cups were transferred to new collection tubes. For elution, 50 µl 2x Reducing Sample Buffer was added to the resin and incubated at room temperature for 2 min. After centrifugation at 6,000 g for 2 min, the spin cup was discarded. The eluted samples were heated for 5 min at 100°C.

4.9.4 SDS-PAGE Gel Electrophoresis

At least 25 µl of heated samples were applied per lane of NuPAGE® 4-12% Bis-Tris gels (Invitrogen). SeeBlue® Plus2 pre-stained standard molecular weight marker (Invitrogen) and MagicMark™ XP western protein standard (Invitrogen) were used as protein standards. Minigels were run in MOPS buffer at 200 V in an electrophoresis system (Novex XCell) (Invitrogen).

4.9.5 Semi-dry transblotting

After separation of the samples on SDS-PAGE, the proteins were transferred to polyvinylidene fluoride (PVDF, 0.45 µm) (Amersham, GE Healthcare, Buckinghamshire, UK) membranes. Gels were carefully removed and equilibrated in transfer buffer for 10 min. Meanwhile, the PVDF membrane was activated by incubation in methanol (Merck) for 1 min followed by incubation in transfer buffer for 10 min. At the same time, blotting paper was soaked in transfer buffer and placed on the lower electrode (anode) of the Semi-Dry SD Transblotter (Bio-Rad). The membrane and the separating gel were placed between two pieces of moist blotting paper. A glass pipette was scrolled over to remove

air bubbles between them. Thereafter, the sandwich was covered with the upper electrode (cathode) and blotted at 15 V for 40-45 min.

4.9.6 Immunodetection / Western Blot Analysis

After protein transfer, the membrane was blocked in TBS containing 3% BSA at room temperature for 2 hours. The membrane was rinsed with TBST for 5 min and incubated in a solution containing the secondary anti-Ras mouse monoclonal antibody-HRP-conjugate (1:10,000) (Amersham Biosciences, Amersham, UK) in 5% nonfat dry milk (Sigma-Aldrich) in at room temperature for 1 hour. The membrane was washed five times for 5 min each with TBST and afterwards incubated in enhanced chemiluminescence solution (ECL) (Amersham Biosciences) for 2 min and was covered with a plastic bag. The blots were exposed to X-ray film (Amersham Hyperfilm ECL) (Amersham Biosciences) for different exposition times. The X-ray films were developed in a dark room with standard reagents (developer and fixer) and dried with warm air. Detected activated Ras-protein of *H-Ras* transfected HaCaT clones was displayed as multiple of the intensity of non transfected HaCaT cells by use of the ImageJ 1.37c software (Wayne Rasband, National Institute of Health, Bethesda, MD, USA).

4.10 Immunohistochemistry

Tissue samples and Matrigel plugs were cut into 5 µm (paraffin) or 8 µm (frozen sections) transversal sections by use of either a microtome (1150/Autocut, Reichert-Jung, Wetzlar, Germany) or cryomicrotome (-30°C) (2800 Figocut E, Reichert-Jung, Wetzlar, Germany), and subsequently mounted on adhesive microscope slides (Thermo Scientific). Paraffin embedded sections were stored at RT. Cryoprotected slides were stored at -80°C. Images were acquired by using a Zeiss Cell Observer (Zeiss Axiovision 4.6 software, Carl Zeiss Microimaging, Göttingen, Germany).

4.10.1 Frozen sections

Tissue sections of frozen Matrigel plugs and of frozen tumor tissues of melanoma, breast cancer and HNSCC patients were air dried and fixed in acetone (Roth) for 5 min. Afterwards, samples were pretreated with 0.6% hydrogen peroxide (Merck) in PBS (PAA) for 10 min at room temperature to quench endogenous peroxidases. Sections of Matrigel plugs were stained with a biotinylated monoclonal rat antibody against murine CD31 (Tab.

2). After incubation of the primary antibody sections were washed in PBS (PAA) and incubated in streptavidin horseradish peroxidase-(HRP) conjugate (Dako, Glostrup, Denmark). Bound antibody was visualized using the Elite-ABC reagent (Vector Laboratories, Inc., Burlingame, CA, USA) with 3-Amino-9-Ethyl-carbazol (AEC) (Vector Laboratories) as a substrate for 5 to 20 min. Following washes, slides were counterstained with hematoxylin (Sigma-Aldrich) for less than 1 min at RT, rinsed in water and permanently mounted in Ultramount Plus (Labvision Products, Fremont, CA, USA). Sections of tumor tissues of melanoma, breast cancer and HNSCC patients were stained against human CCL20 or against human pERK (Tab. 2) according to the accomplishment of CD31 staining of frozen Matrigel plugs.

4.10.2 Paraffin sections

Paraffin embedded sections were deparaffinized in xylene (Merck) and rehydrated in decreasing series of ethanol (Merck). Sections were finally washed in PBS (PAA) and, in case of staining against CCL20, unmasked by incubation in Proteinase K (1:50 in 0.05 M Tris-HCl pH 7.5) (Dako) for 15 min at room temperature. In case Of staining against pERK sections were unmasked by boiling in Target Retrival Solution (1:10 in dH_2O; Dako) for 10 min. Unmasking steps were followed by incubation in 0.3% hydrogen peroxide (Merck) in PBS (PAA) for 30 min. In order to block non-specific binding sites sections were incubated for 1 hour in 10% normal rabbit serum (AbD Serotec, Düsseldorf, Germany). For immunohistochemical analyses of tumor tissue microarrays, paraffin sections were stained with biotinylated antibodies against human CCL20 or human pERK (Tab. 2). Paraffin embedded mice tumors were stained against murine CD31 (Tab. 2). Slides were rinsed in PBS (PAA) in order to remove unbound antibody, and subsequently incubated in streptavidin horseradish peroxidase-(HRP) conjugate (Dako). In case of CCL20 and pERK bound antibody was visualized using the Elite-ABC reagent (Vector Laboratories, Inc.) with 3-Amino-9-Ethyl-carbazol (AEC) (Vector Laboratories, Inc.) as a substrate according to the manufacturer's instructions. In case of CD31, mice tumors were treated with HistoGreen (HistoGreen Substrate Kit for Peroxidase, Linaris Histoprime®, Wertheim-Bettingen, Germany) according to the manufacturer’s instructions. Following washes slides were counterstained with hematoxylin (Sigma-Aldrich) for less than 1 min at RT, rinsed in water, and permanently mounted in Ultramount Plus (Labvision Products, Fremont, CA, USA).

Table 2: List of different primary antibodies, isotype controls and corresponding dilutions. Antibodies are diluted in PBS (PAA).

Primary Antibody	Dilution / Incubation time	Company
Monoclonal rat anti-mouse CD31, ER-MP12, IgG2a	35 µg/ml (1:17) , over night at 4°C	Acris Antibodies, Herford, Germany
Polyclonal goat anti-human CCL20, IgG	15 µg/ml (1:3) , 90 min at 37°C	R&D Systems, Minneapolis, MN, USA
Monoclonal mouse anti human phosphor-p44/42 MAPK (Erk1/2) Thr202/Tyr204), E10, IgG1	1:10 in 0.03% Triton® X-100 (Roth), 90 min at RT	Cell Signaling, Danvers, MA, USA
Isotype control IgG2a		BD Biosciences, San Jose, CA, USA
Isotype control IgG		Santa Cruz Biotechnology, Inc., Santa Cruz, CA, USA
Isotype control IgG1		BD Biosciences

4.11 Immunofluorescence

BECs and LECs were seeded on Lab-Tek® 2 well glass chamber slides (Nalge Nunc International, Rochester, NY, USA) and cultured to 80% confluence. Cells were fixed with a mixture of methanol and acetone (all Merk) (3:1) and stained against human CCR6 with a phycoerythrin (PE)-labeled antibody (BD Pharmingen, San Diego, CA, USA; Tab. 3). Cell Nuclei were stained with DAPI (Invitrogen) (1:400) for 15 min at room temperature.

Frozen 8-µm tumor tissue sections were double stained against human CCR6 and human CD31. First tissue sections were fixed in 4% paraformaldehyde (Sigma) and stained against human CCR6 (R&D Systems; Tab. 3) in 2% donkey serum (AbD Serotec). Secondary donkey anti-mouse IgG labeled with Northern Lights (R&D Systems) (1:250) was added for 45 min at room temperature after washing with PBS (PAA). Second, Alexa 488 labeled anti-human CD31 (BD Pharmingen; Tab. 3) was added after blocking with

15% mouse serum (AbD Serotec). All cells were additionally stained with DAPI (Invitrogen) (1:400) for 15 min.

Slides were covered with Fluoromount-G (SouthernBiotech, Birmingham, AL, USA) and cover slips. Immunofluorescent stainings were detected by use of a microscope (Axiovert 200M) (Zeiss) using the software Axiovision 4.7 (Zeiss).

Table 3: List of different primary antibodies, isotype controls and corresponding dilutions.

Antibody	Dilution / Incubation time	Company
Monoclonal mouse anti-human CCR6, 11A9, IgG1	20 µg/ml (1:10), 120 min at 4°C	BD Pharmingen
Monoclonal mouse anti-human CCR6, 53103, IgG2b	20 µg/ml (1:25), over night at 4°C	R&D Systems
Monoclonal mouse anti-human CD31, M89D3, IgG2aκ	20 µg/ml (1:10), 120 min RT	BD Pharmingen
Isotype control IgG1		BD Pharmingen
Isotype control IgG2b		R&D Systems
Isotype control IgG2aκ		BD Pharmingen

4.12 *In vitro* monolayer wound healing assay

BECs (Lonza) were cultured to confluence in 24-well plates. Scratch wounds were introduced in the monolayers by using a sterile 0.1–10 µl pipette tip. After washing away suspended cells, cultures were supplied with cell medium containing 0 or 100 ng/ml recombinant CCL20 (R&D Systems). This was set as time point zero (t=0). Images of the same area were taken under bright field at t=0 and after an incubation time of 18 hours. Imaging was performed with a Zeiss Cell Observer (Zeiss).

4.13 Tube formation assay

Growth factor reduced Matrigel (BD Biosciences) was thawed over night at 4°C and 10 µl of ice cold Matrigel were pipetted per well in µ-slide angiogenesis chambers (ibidi, Munich, Germany) and incubated for 45 min at 37°C for polymerization. 2 x 10^3 BECs in EGM-2MV supplemented with 5% FCS (Clonetics) and with 0, 10, 100 or 1,000 ng/ml of recombinant CCL20 (R&D Systems) were seeded on top. Cells were incubated in an incubator at 37°C with 95% humidity and 5% CO_2 (INCO 2: Memmert). Observed tube formation was imaged after 6 hours of incubation with a Zeiss Cell Observer (Zeiss). Tube formation was quantified by counting the number of junctions of at least three tubes (termed node) per well.

4.14 Chemotactic cell migration

Chemotactic cell migration was performed according to the µ-slides chemotaxis manual (ibidi) using collagen coated chemotaxis µ-slides. BECs were seeded into observation chambers at a density of 1 x 10^6 cells/ml. CCL20 (R&D Systems) and CCL21 (R&D Systems) gradients were generated at 1,000 to 10 ng/ml. In controls, cells were pre-treated with 30 µg/ml anti human CCR6 (R&D Systems) for 10 min and anti human CCR6 was supplied to the assay. Cells were observed for 60 hours with a Zeiss Cell Observer (Zeiss). To analyze cell migration, movement of cells during observation time was tracked using ImageJ 1.37c software (Wayne Rasband, National Institute of Health). Starting points of cell migration trajectories were set to the origin of a coordinate system and x- and y- values of the endpoints were used for further analysis of cell movement behavior. ΔY, the distance of cells traveled along the chemokine gradient (Y-axis), and the percentages of endothelial cells traveled in the direction of chemokine gradients (Y-axis) $\Delta Y < 0$ were calculated. Values above 50% show a tendency of cell movement in direction of higher chemokine concentrations. Further percentages of endothelial cells traveling a longer distance in the direction of chemokine gradients (Y-axis) than in the direction orthogonal to the gradients (X-axis) $\Delta Y / |\Delta X| < -1$ were determined. Values higher than 25% indicate a directed migration of cells in direction to higher concentrations of the chemokine gradient.

4.15 Enzyme-linked immunosorbent assay (ELISA)

Quantification of CCL20 concentration in cell culture supernatants was performed according to the DuoSet ELISA Development kit protocol (R&D Systems). In detail, a 96-well microplate (Nunc) was coated with 2 µg/ml of monoclonal capture antibody and incubated overnight at room temperature. Plates were than blocked with reagent diluent (1% BSA (Sigma-Aldrich®) in PBS (PAA)) for 1 hour at room temperature, washed with wash buffer (0,05% Tween-20 (Bio Rad, München, Germany) in PBS (PAA)) and filled with samples and standards (2,000 pg/ml to 31,25 pg/ml recombinant human CCL20). Samples and standards were incubated 2 hours at room temperature. This was followed by another wash step and the addition of biotinylated goat anti-human CCL20 detection antibody (50 ng/ml) for 2 hours at room temperature. After a further wash step a working solution of streptavidin conjugated to horseradish-peroxidase was filled in the wells and incubated for 20 min at room temperature to bind to the biotinylated detection antibody. An additional wash step was followed by incubation of the wells with a substrate solution (1:1 mixture of color reagent A (hydrogen peroxide) and color reagent B (Tetramethylbenzidine)) (Substrate reagent pack; R&D Systems) for 20 min at room temperature. Finally, stop solution (1 M H_2SO_4 was added. Optical densities were measured at 450 nm by use of a microplate reader (MR 5000, Dynatech Laboratories, Inc., Alexandria, Va.).

For absolute quantification of CCL20 protein in cell supernatants, standard curves lines were prepared:

$$x = (y - b)\, m^{-1}$$

Where x is the protein concentration of interest in pg/ml. y is the absorption of the sample at 450 nm. m is the slope and b is the Y-axis intercept of the standard curve line.

4.16 Flow cytometric analysis (FACS)

BECs and LECs (all Lonza) were analyzed using flow cytometry. Cells were harvested by treatment with accutase (PAA) for 5 min at 37°C and centrifuged (220 g, 10 min, RT) (Rotanta 46 RC, Hettich Zentrifugen, Mülheim an der Ruhr, Germany). 10^6 cells were stained with monoclonal anti-human Podoplanin (mouse IgG1, clone D2-40: Dako) for 45

min on ice. After a wash step with PBS (PAA) a FITC-labeled secondary goat anti-mouse IgG (Dako) was added for 30 min at 4°C. Samples were kept in the dark. After washing again with PBS (PAA) cells were blocked with 15% mouse serum (Pel-Freez Biologicals, Rogers, AR, USA) for 30 min at 4°C and stained with PE-labeled monoclonal anti-human CCR6 (mouse IgG1, clone 11a9: BD Pharmingen) for 45 min at 4°C. After a wash step with PBS (PAA) cells were fixed in 1% paraformaldehyde (Merck) and then analyzed with a FACSCalibur flowcytometer and CellQuest software (all BD Biosciences). At least 30,000 events were counted. Data was analyzed by a histogram plot (counts over fluorescence). To determine non specific stainings the unlabeled monoclonal mouse IgG1 (isotype control for Podoplanin: R&D Systems) and PE-labeled mouse IgG1 (isotype control for CCR6: BD Pharmingen) were used. Cells were initially gated on the basis of forward scatter (FSC) and side scatter (SSC) characteristics with gates set to remove dead cells.

4.17 Matrigel plug assay

Growth factor reduced Matrigel (BD Biosciences) was thawed over night at 4°C. Ice cold Matrigel was gently mixed with 1,000 ng/ml recombinant murine CCL20, 1,000 ng/ml recombinant human CCL21 (all R&D Systems) or PBS (PAA) as a negative control. 500 µl of Matrigel was injected subcutaneously in the lateral flanks of wild-type-C57BL/6-mice (Taconic) and C57BL/6-CCR6$^{-/-}$-mice (S. Lira) with a syringe. After extraction of the needle, the puncture site was compressed for 10 seconds until Matrigel was polymerized to avoid efflux. To allow vascularization of the Matrigel, plugs remained in mice for 21 days. After three weeks, mice were sacrificed and Matrigel plugs were removed and immediately snap frozen in liquid nitrogen. Neovascularization in plugs was analyzed by immunohistochemistry.

4.18 Murine syngeneic tumor model B16/F10

Flat-panel detector volume computed tomography (fpVCT) allows three-dimensional (3D) visualization of murine anatomic structures and allows a detailed visualization of the skeleton of mice. With a resolution of 150 to 200 µm it is an ideal method to monitor tumor-infiltrating vessels in living animals. In this experiment 2.5 x 10^5 B16/F10 cells (ATCC) in a total volume of 100 µl of PBS were injected subcutaneously in the lateral right

flank of wild-type-C57BL/6-mice (Taconic) and C57BL/6-CCR6$^{-/-}$-mice (S. Lira) with a syringe. After tumor growth for 14 days mice were imaged by fpVCT (GE Global Research, Niskayuna, NY, USA), a nonclinical volume CT prototype. Before imaging and throughout the imaging session mice were anesthetized with vaporized isoflurane at 0.8% to 1% concentration. An iodine-containing contrast agent, Ultravist 150 (at 150 µl per mouse: Bayer-Schering, Berlin, Germany), was applied intravenously approximately 30 seconds before scan. At the end of the experiment mice were sacrificed and tumors were excised, weighed, paraffin embedded and analyzed by immunohistochemistry. Additionally tumor volume was calculated. Imaging was performed with kind support of Prof. Dr. Frauke Alves' group (department hematology and oncology, Georg-August-Universität, Göttingen, Germany).

4.19 Statistic analysis

Statistical analyses were calculated using nonparametric Mann-Whitney U test. To test the correlation between the clinico-pathological data and the level of CCL20 expression as well as correlation between pERK expression and CCL20 expression the Fisher's exact test was used and whenever appropriate the χ^2-test. All of the variables were dichotomised. For analysis of follow-up data, life table curves were calculated using the Kaplan-Meier method, and survival distributions were compared using the log-rank test. The primary end points were disease-specific survival or relapse-free survival, as measured from the date of surgery to the time of the last follow-up or cancer-related death. Variations were considered to be statistically significant at values of $P<0.05$. P-values < 0.05 are indicated by *, < 0.005 by ** and p-values < 0.001 by ***.

5 Results

5.1 CCL20 is highly induced by Ras activation

Persistent activation of the oncogene Ras is a hallmark of numerous malignant transformations of cells. To identify chemokines regulated by Ras activation, the gene expression of chemokines in normal HaCaT keratinocytes and in HaCaT keratinocytes transfected with the activated H-RasV12 oncogene was analyzed (Fig. 4). Interestingly the expression of all investigated chemokine genes showed a clear correlation with the activation of H-Ras protein. Thus *CXCL14* was identified as a gene whose expression is downregulated by Ras activation (Fig. 4B), and the Ras-dependent downregulation of *CCL27* (Fig. 1C) was confirmed[104]. In contrast, another set of chemokine genes was upregulated by Ras activation, namely *CCL20* and *CXCL8* (Fig. 4D-E). *CXCL8* expression has already been described as being ERK-induced[110,111]. However, *CCL20* showed the highest upregulation in correlation to Ras activation among all the tested chemokines. This result required that Ras dependent expression of CCL20 had to be investigated into further detail.

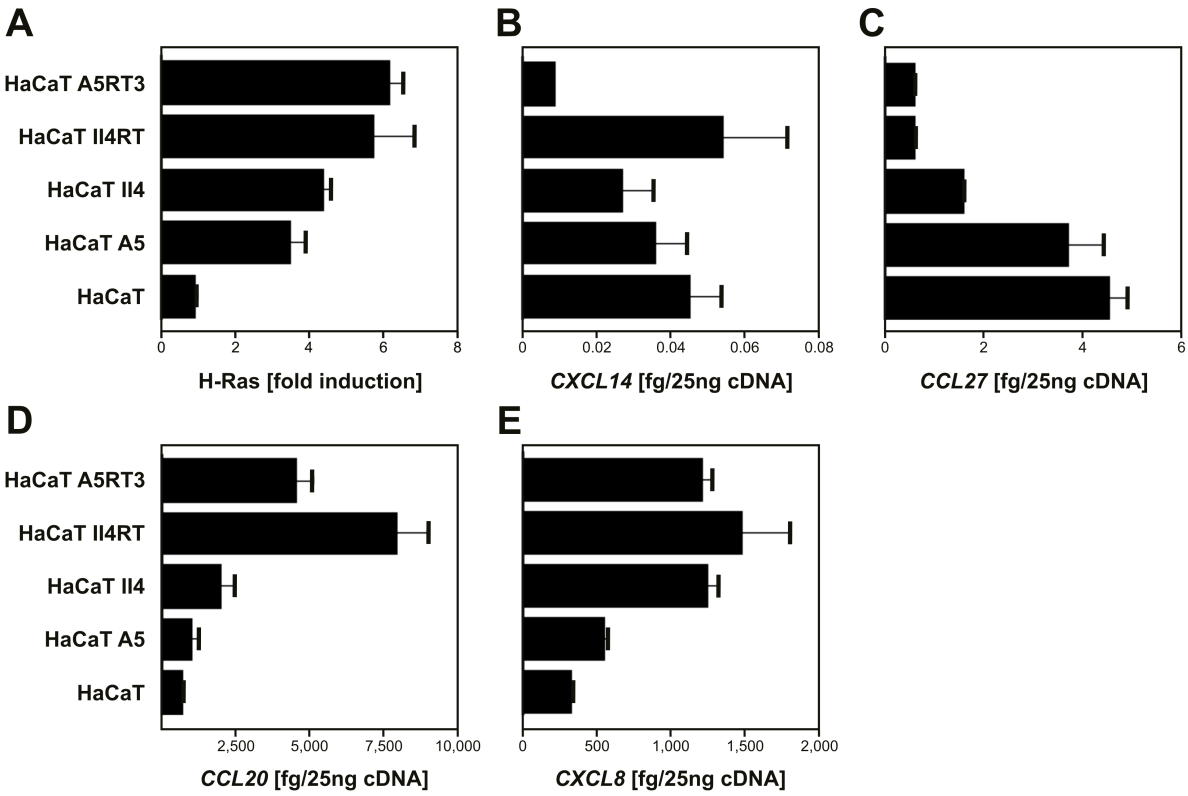

Fig. 4: Oncogenic Ras induces *CCL20* and *CXCL8* gene expressions whereas gene expression of *CCL27* and *CXCL14* is repressed. (**A**) Relative Ras activity in the immortalized keratinocyte cell line HaCaT and in H-Ras-transfected HaCaT clones were assayed by the Active Ras Pull-Down and Detection Kit. (**B-E**) *CXCL14*, *CXCL8* and *CCL20* mRNA expression of untransfected HaCaT cells and of H-Ras-transfected HaCaT clones was analyzed by qRT-PCR. Values are expressed as femtograms of target gene per 25 ng of cDNA and represent the mean ± SD of three independent experiments.

5.2 The EGFR/Ras signaling pathway regulates CCL20 gene and protein expression

The CCL20 chemokine expression in H-RasV12-transfected HaCaT keratinocytes was analyzed (Fig. 5A). At the mRNA level a CCL20 overexpression in response to Ras activation was detected (Fig. 5B). These data were confirmed at the protein level by examining CCL20 secretion into cell culture supernatants of HaCaT H-RasV12 clones with high Ras activity (HaCaT II4RT and HaCaT A5RT3) using ELISA (Fig. 5C). These findings indicate that *CCL20* mRNA expression directly translates into protein secretion by the cells. To test whether the observed induction of *CCL20* expression is dependent on EGFR activation, EGFR signaling in keratinocytes was blocked with the specific inhibitor

erlotinib[112,113,114] and *CCL20* expression was analyzed after 24 hours. In response to EGFR inhibition, a significant reduction in *CCL20* expression was observed at both the mRNA and protein levels (Fig. 5D-E), indicating that *CCL20* expression is controlled by the EGFR/Ras signal transduction pathway.

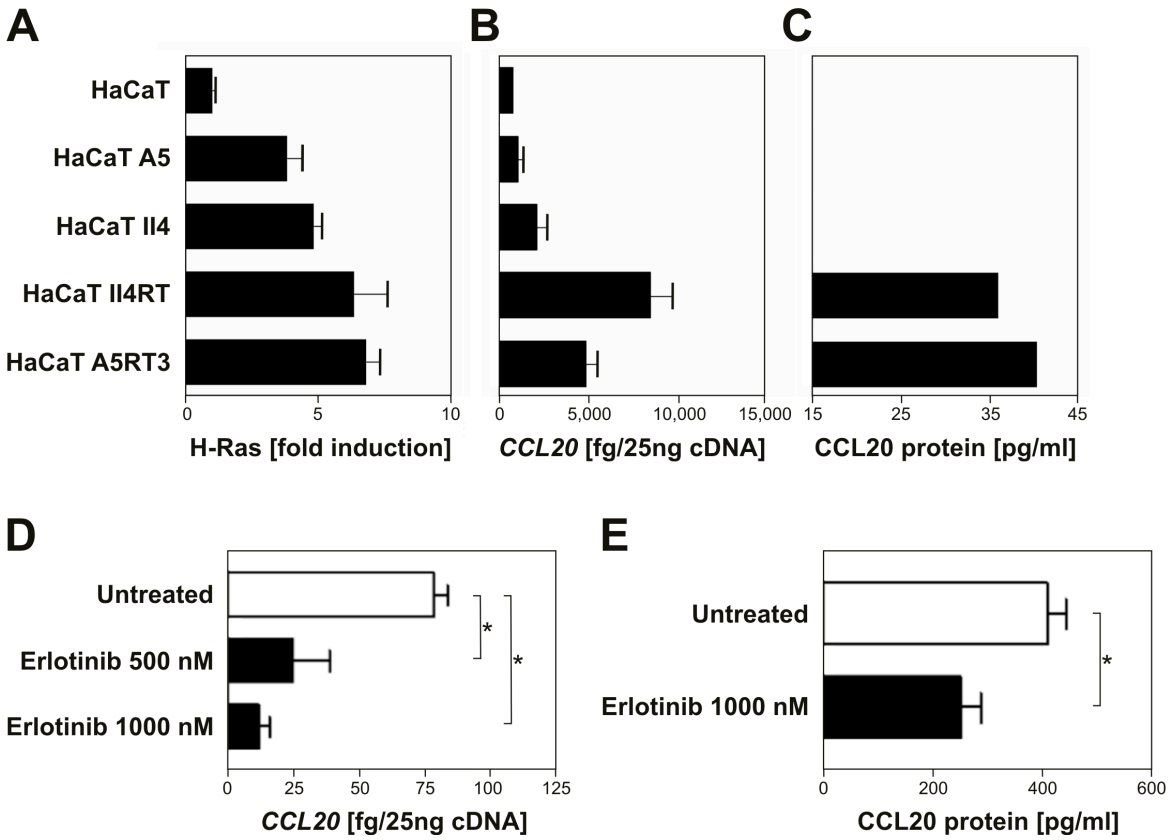

Fig. 5: Oncogenic Ras induces *CCL20* transcription and protein synthesis. (**A**) Relative Ras activity in the immortalized keratinocyte cell line HaCaT and in H-Ras-transfected HaCaT clones were assayed by the Active Ras Pull-Down and Detection Kit. (**B**) *CCL20* mRNA expression of untransfected HaCaT cells and of H-Ras-transfected HaCaT clones was analyzed by qRT-PCR. Values are expressed as femtograms of target gene per 25 ng of cDNA and represent the mean ± SD of three independent experiments. (**C**) CCL20 protein production of HaCaT cells and H-Ras-transfected HaCaT clones as detected by a specific ELISA system in supernatants of cell culture. Values are expressed as pg of protein per ml of supernatant. (**D-E**) Activated primary keratinocytes were treated with Erlotinib, a selective irreversible inhibitor of EGFR tyrosine kinase. Gene expression of *CCL20* was analyzed by qRT-PCR (**D**) and CCL20 protein expression by a specific ELISA system (**E**). Values are either expressed as femtograms of target gene per 25 ng of cDNA or as protein concentration and represent the mean ± SD of three independent experiments (**, P≤0.01; ***, P≤0.001; Mann-Whitney U test).

5.3 CCL20 expression is induced in several cancer types

Since EGFR/Ras-dependent expression of CCL20 was observed in HaCaT keratinocytes, CCL20 expression was determined in tumor cell lines from breast cancer (n=8), melanoma (n=12) as well as head and neck squamous cell carcinoma (HNSCC) (n=14). A high CCL20 expression was noted in the cancer cells when compared to the corresponding benign precursor cells, namely mammary epithelial cells, melanocytes, and mucosal keratinocytes, respectively (Fig. 6A-C). In comparison to mammary epithelial cells, *CCL20* expression was high in MDA-MB-468 and MDA-MB-361, was comparable in MCF-7, T-47D and MDA-MB-435S and was lower in DU-4475, Hs578T, and MDA-MB-435P breast cancer cells (Fig. 6A). All analyzed melanoma cell lines exhibited high expression of *CCL20* compared to melanocytes, which express *CCL20* only at very low levels (Fig. 6B). With the HNSCC cell lines, half of the analyzed lines (UD-6, UD-7A, UD-7B, UM-10B, UM-17A and B, as well as UT-24B) expressed very high *CCL20* mRNA levels, while the others exhibited a comparable or slightly lower expression of *CCL20* compared to mucosal keratinocytes (Fig. 6C). To correlate the observed *CCL20* mRNA levels with protein expression, CCL20 protein levels were investigated in supernatants from HNSCC, melanoma and breast cancer cell lines using ELISA (Fig. 6D). CCL20 was present in all analyzed supernatants, indicating that *CCL20* mRNA expression corresponds directly to CCL20 protein secretion.

Next *CCL20* expression was investigated in tumor biopsies taken from patients suffering from breast cancer, melanoma, and HNSCC. Significantly higher expression of *CCL20* was observed in breast cancer metastases compared to healthy mammary tissue (Fig. 6E). In comparison to melanocytes, primary melanoma showed an increased *CCL20* expression that was even higher in subcutaneous metastases (Fig. 6E). In HNSCC, significantly increased *CCL20* expression was observed in primary tumor tissue compared to normal mucosa (Fig 6E). In conclusion, a robust enhanced expression of CCL20 was observed in the majority of tested cancer cell lines and tumor samples compared to the corresponding benign precursor cells.

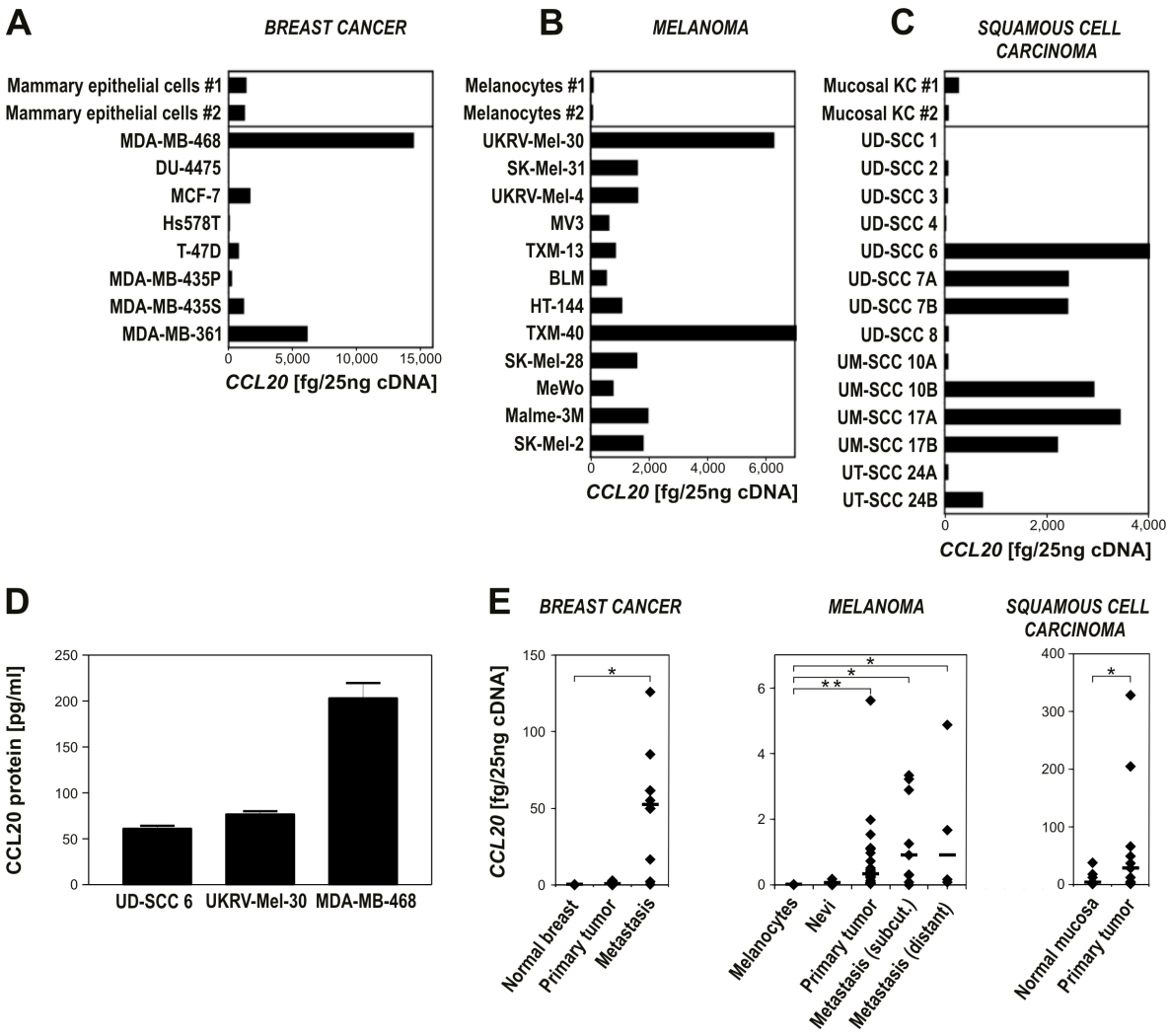

Fig. 6: Tumor cells derived from breast cancer, malignant melanoma and head and neck squamous cell carcinoma (HNSCC) overexpressed *CCL20*. (**A-C**) Quantitative real-time PCR analysis of *CCL20* in cultured normal primary mammary epithelial cells (n=2) and breast cancer cell lines (n=8) (**A**), cultured normal primary melanocytes (n=2) and melanoma cell lines (n=12) (**B**), cultured primary mucosal keratinocytes (KC; n=2), cell lines derived from primary tumors (n=10) or metastases (n=4) of head and neck squamous cell carcinoma (**C**). (**D**) CCL20 protein expression in supernatants of squamous cell carcinoma (UD-SCC6), melanoma (UKRV-Mel-30) and breast cancer (MDA-MB-468) cell lines. Values are expressed in picograms per ml of supernatant. (**E**) Quantitative real-time PCR analysis of *CCL20* in tumor tissues derived from breast cancer (primary breast cancer, n=12 and breast cancer metastasis, n=10), malignant melanoma (primary melanoma, n=28, subcutaneous metastasis, n=11 and distant metastasis, n=4) and head and neck squamous cell carcinoma (primary tumor, n=14) compared to normal tissue (normal breast, n=3, cultured primary melanocytes, n=3, benign nevi, n=5 and normal oral mucosa, n=8). Values are expressed as femtograms of target gene in 25 ng of total cDNA (*, P≤0.05; **, P≤0.01; Mann-Whitney U test).

5.4 CCL20 expression of tumor tissues correlates with ERK activation, advanced cancer staging and poor prognosis

As tumor tissues express *CCL20* at the mRNA level (Figure 6E) and EGFR/Ras signaling upregulates CCL20 expression (Fig. 5), next immunohistochemical analysis of CCL20 expression was performed in tumor samples from breast cancer, melanoma and HNSCC patients, and compared this with ERK activation (Fig 7A). Interestingly, sites of strong ERK activation corresponded to sites of strong CCL20 expression (Fig. 7A). Next further samples were analyzed using tumor tissue microarrays of breast cancer, HNSCC and colon carcinoma tumors. CCL20 expression and the presence of pERK were again analyzed by immunohistochemical staining (Fig. 7B). The samples were categorized as expressing CCL20 at either high ($CCL20^{high}$) or low levels ($CCL20^{low}$), and also whether they exhibited high activation of pERK ($pERK^{high}$) or low pERK activation ($pERK^{low}$). In 121 cases of breast cancer and HNSCC, high ERK phosphorylation levels were observed in 84.5 % of $CCL20^{high}$ tumors but in only 51% of $CCL20^{low}$ expressing tumors ($P<0.001$; Pearson's chi-square test) (Tab. 4). These data therefore show a highly significant correlation between CCL20 expression and activated ERK.

CCL20 expression was also examined in relation to tumor grade. In 334 cases of breast cancer, colon carcinoma and HNSCC, a higher pT-category of the observed tumors correlated significantly to higher expression of CCL20 ($P=0.004$; Pearson's chi-square test) (Tab. 5). CCL20 expression and pN-category showed a less pronounced correlation, which nevertheless was still statistically significant ($P=0.048$; Pearson's chi-square test) (Tab. 5). Taken together, these data demonstrate that CCL20 expression correlates to ERK activation, and that tumors expressing high levels of CCL20 have a more aggressive phenotype.

Next the expression of CCL20 was analyzed in a breast cancer tumor tissue microarray containing tumor tissues from 40 different patients for whom follow-up data was available. Cumulative survival in the $CCL20^{low}$ group after 80 months was 93%, while cumulative survival in the $CCL20^{high}$ group was significantly lower at 70% ($P=0.05$) (Fig. 7C). Thus, high CCL20 expression in primary breast tumors significantly reduces cumulative survival of the patients after tumor excision. Together these results suggest that tumor-derived CCL20 promotes tumor progression and growth, and has a corresponding negative effect on the survival of breast cancer patients.

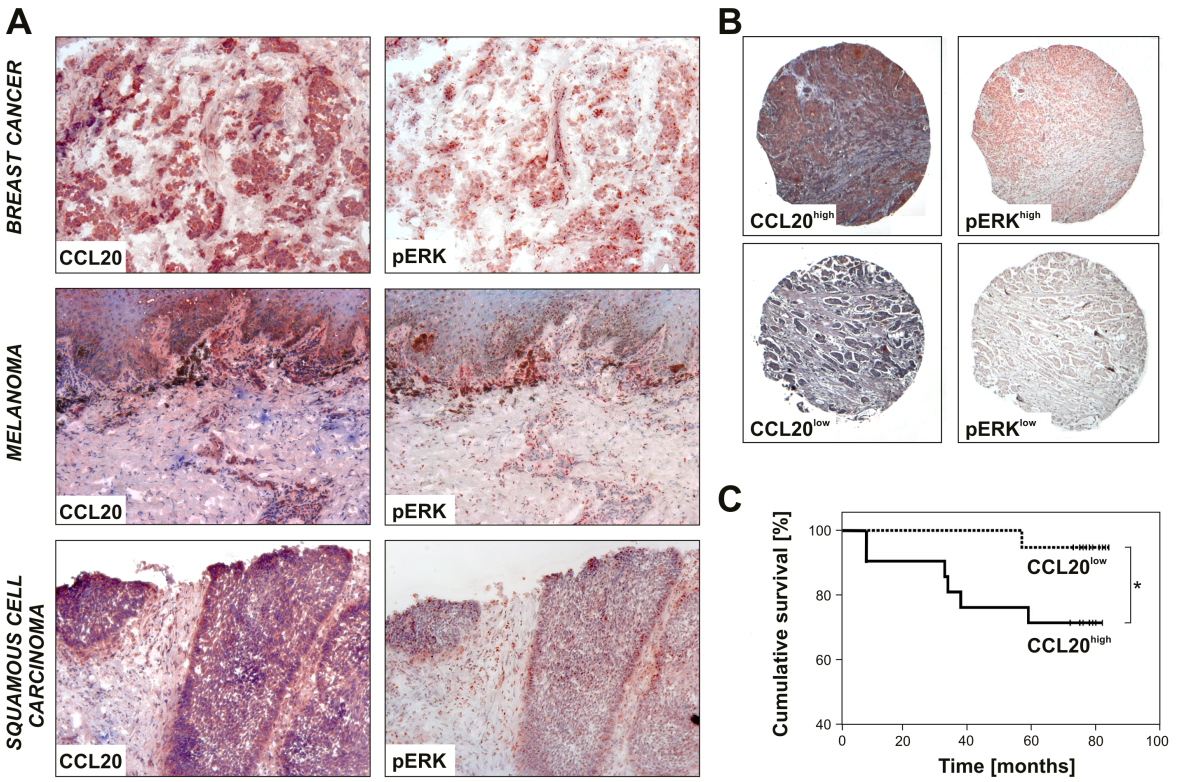

Fig. 7: Tumor-derived CCL20 production co-localizes to areas of ERK activation and correlates to progressive states of cancer. (**A**) Representative results of serial sections of breast cancer (n=6), melanoma (n=6) and HNSCC (n=6) stained with anti-CCL20 or anti-pERK1/2 antibodies are shown (magnification 100x). (**B**) Representative high and low expression of CCL20 and pERK in tumor tissue microarrays of breast cancer. Classifications of $CCL20^{high}$, $CCL20^{low}$, $pERK^{high}$ and $pERK^{low}$ were used for further statistical evaluation of tumor tissue microarrays. (**C**) Kaplan-Meyer graph showing cumulative patient's survival of breast cancer patients as a percentage to follow-up time in month. Statistical analyses were performed by Chi-Square test using SPSS software (*, P≤0.05; Mann-Whitney U test).

Table 4: Correlation of CCL20 and pERK expression

	# of cases*	$pERK^{low}$[%]	$pERK^{high}$[%]	*P* value
Total	121			<0.001
$CCL20^{low}$ expression	63	49.2	50.8	
$CCL20^{high}$ expression	58	15.5	84.5	

* 73 breast cancer tissues and 48 HNSCC tissues were analyzed for CCL20 expression and ERK activation. Expressions were correlated and statistically analyzed by Pearson's Chi-Square test using SSPS software.

Table 5: Correlation of tumor entity and CCL20 expression

	# of cases*	$CCL20^{low}$[%]	$CCL20^{high}$[%]	*P* value
Total	334			0.004
pT1	15	46.7	53.3	
pT2	111	31.5	68.5	
pT3	157	16.6	83.4	
pT4	51	31.4	68.6	
Total	338			0.048
pN0	219	27.9	72.1	
pN1	64	15.6	84.4	
pN2	50	20.0	80.0	
pN3	5	60.0	40.0	

* Tissue Microarrays of colon carcinoma (n=213), breast cancer (n=73) and HNSCC (n=48) were analyzed for CCL20 expression. Expression data was correlated to TNM values (T=tumor size; N=degree of spread to regional lymph nodes) and statistically analyzed by Pearson's Chi-Square test using SPSS software.

5.5 Endothelial cells express the CCL20-specific chemokine receptor CCR6

Next it was investigated how tumor-derived CCL20 functionally promotes tumor progression, growth and poor prognosis. It was hypothesized that tumor-derived CCL20 acts on a tumor promoting microenvironment. Given that the vasculature plays a major role in regulating tumor growth, it was investigated whether microvascular endothelial cells express CCR6, the corresponding receptor for CCL20, on their surface. In FACS analyses, abundant CCR6 expression was observed on podoplanin-negative human blood microvascular endothelial cells (BEC) and on podoplanin-positive human lymphatic microvascular endothelial cells (LEC) (Fig. 8A). Additionally, strong staining for CCR6 inside the cells as well as on the cell surface of BEC and LEC could be detected using immunofluorescence (Fig. 8B). Furthermore, it was found that vessels in the vicinity of CCL20-positive tumor tissues expressed CCR6. Tissue sections of breast cancer and melanoma were double-stained for CD31 and CCR6 in immunofluorescence experiments. CD31/CCR6-positive vessels were found in proximity to tumors in breast cancer and melanoma samples (Fig. 8C). The fact that CCR6-positive vessels are closely apposed to CCL20-expressing tumors allowed us to hypothesize that CCL20 might be able to functionally activate the microvasculature and induce angiogenesis.

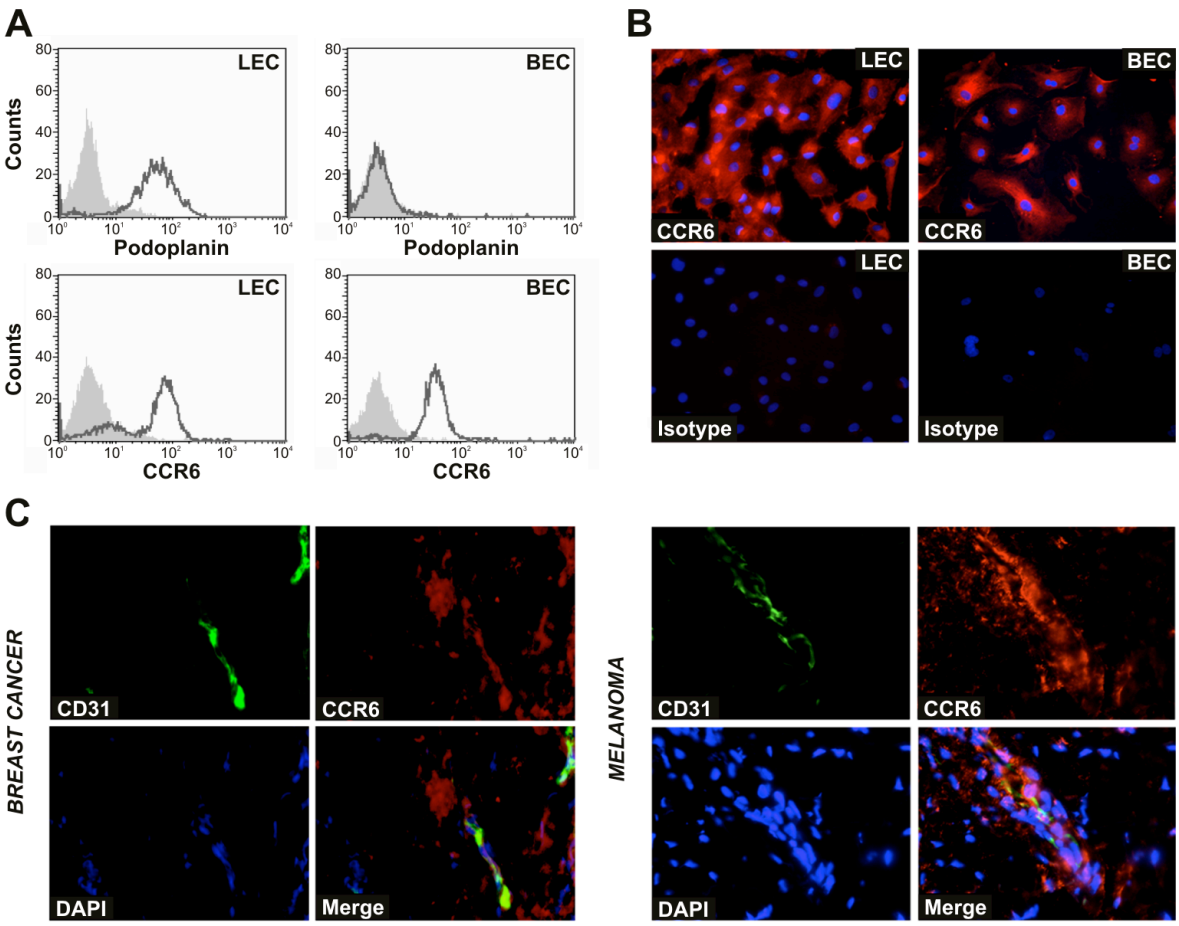

Fig. 8: Microvascular endothelial cells express CCR6 on their cell surface. (**A**) Flow cytometric analysis of podoplanin and CCR6 protein surface expression in podoplanin-positive lymphatic microvascular endothelial cells (LEC) or podoplanin-negative blood microvascular endothelial cells (BEC) (black lines). Filled histogram shows isotype control. (**B**) Immunofluorescence analysis of CCR6 (red) expression of LECs and BECs (magnification 400x). (**C**) Immunofluorescence analysis of CD31 (green) and CCR6 (red) expression in marginal zones of a breast cancer tumor and melanoma demonstrates the co-localization of CCR6 with CD31 positive microvessels in the tumor microenvironment (magnification 200x).

5.6 CCL20 promotes the migration of microvascular endothelial cells and tubule formation *in vitro*

To test the hypothesis that tumor-derived CCL20 might participate in tumor-induced angiogenesis, the effect of CCL20 on microvascular endothelial cells was investigated *in vitro*. Chemotaxis assays were performed using IBIDI µ chemotaxis slides. Ibidi µ chemotaxis slides were combined with computer-assisted videomicroscopic motion analyses to obtain trajectories made by motile BEC (Fig. 9A). Subsequently, BEC trajectories were statistically analyzed relative to the direction of the chemical gradient using an established directionality-based assay, independent of BEC motility speed and pattern of movement and therefore measuring chemotaxis only (Fig. 9B-D). The strongest chemotactic response was observed with CCL20 gradients, while response rates obtained with the irrelevant chemokine CCL21 or with medium were equivalent to values expected for randomly moving cells showing no chemotaxis (Fig. 9A-D). Furthermore, chemotaxis of BEC towards CCL20 was significantly impaired using neutralizing anti-human CCR6 antibodies, suggesting an important role for CCL20-CCR6 interactions in guiding BEC. The motility-enhancing effect of CCL20 was further substantiated in monolayer wound repair assays. At doses of 100 ng/ml, CCL20 induced faster monolayer wound closure than control medium alone (Fig. 9E).

Another facet of the angiogenic response is the induction of capillary tube formation by endothelial cells. The ability of CCL20 to influence tube formation was assayed *in vitro* by plating endothelial cells on Matrigel and treating them with varying concentrations of CCL20 (100 – 1,000 ng/ml), or with PBS as a control. Three independent experiments were performed and the data were analyzed by counting nodes of three or more tubes. In the control, 50 (SD ± 7) nodes were observed. Significantly more nodes were induced by CCL20, as 10 ng/ml CCL20 induced 70 (SD ± 16), 100 ng/ml CCL20 induced 70 (SD ± 8) and 1,000 ng/ml CCL20 induced 66 (SD ± 12) nodes per well (Fig. 9E). It was therefore concluded that CCL20 is able to enhance aspects of endothelial cell angiogenesis.

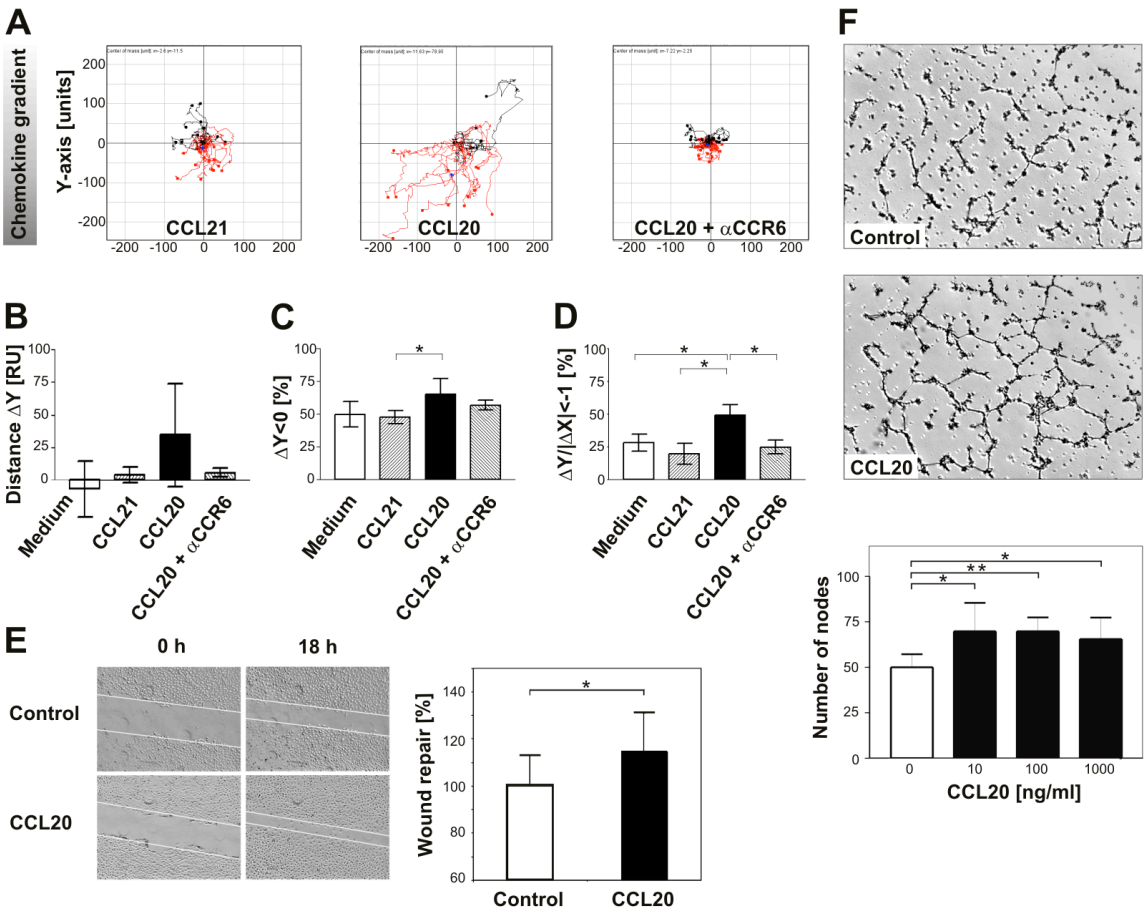

Fig. 9: CCL20 mediates directional migration of human microvascular endothelial cells and enhances tube formation. (**A**) Representative trajectories of microvascular endothelial cells cultured inside an IBIDI µ chemotaxis chamber containing chemokine gradients of CCL20 (0 to 1,000 ng/ml), CCL21 (0 to 1,000 ng/ml; irrelevant chemokine control), or endothelial cells pre-incubated with anti-CCR6 antibodies (30 µg/ml) and cultured in slides containing CCL20 (0 to 1,000 ng/ml). Trajectories are representatives for test and control stimuli of at least 3 different experiments. (**B-D**) Statistical analysis of endothelial cell trajectories. (**B**) Average ΔY, mean net distance (RU) of cells traveled along the chemokine gradient (Y-axis). (**C**) ΔY < 0, Percentages of endothelial cells traveling in the direction of chemokine gradients (Y-axis). Values above 50% show a tendency of cell movement in direction of higher chemokine concentrations (*, P≤0.05; Mann-Whitney U test). (**D**) ΔY / IΔXI < -1, Percentages of endothelial cells traveling a longer distance in the direction of chemokine gradients (Y-axis) than in the direction orthogonal to the gradients (X-axis). Values higher than 25% indicate a directed migration of cells in direction to higher concentrations of the chemokine gradient (*, P≤0.05; Mann-Whitney U test). (**E**) In wound repair assays, CCL20 was able to induce significant wound repair and migration of microvascular endothelial cells when compared to corresponding controls (*, P≤0.05; Mann-Whitney U test). (**F**) Tube formation assay showing representative images of microvascular endothelial cells grown on Matrigel and supplemented with CCL20 (10 ng/ml) or without chemokine. Number of nodes per field are shown and represent the mean ± SD of three independent experiments (*, P≤0.05; **, P≤0.01; Mann-Whitney U test).

5.7 CCL20 enhances vascularization of Matrigel plugs and tumors

After establishing the effect of CCL20 on endothelial cells *in vitro*, it was investigated to reproduce this effect *in vivo*.

5.7.1 CCL20 recruits CD31-positive vessels into Matrigel plugs *in vivo*

To determine whether CCL20 influences angiogenesis *in vivo*, the effect of CCL20 was examined on the growth of blood capillaries in subcutaneous Matrigel plugs. Plugs consisting of Matrigel alone, as well as plugs containing murine CCL20 and human CCL21, were injected into C57BL/6 and CCR6-deficient C57BL/6 mice. Human CCL21 was used as an irrelevant chemokine, because murine CCL21 is able to bind to CXCR3[115]. Endothelial cells express CXCR3 on their cell surface, and murine CCL21 therefore exerts an angiostatic effect[115]. Human CCL21, on the other hand, has been demonstrated to bind to mouse CCR7 but not to murine CXCR3[116], and therefore represents a suitable control for this experiment. After excision, plugs were analyzed for the number of CD31-positive vessels (Fig. 10A). In control plugs from wild-type and CCR6-deficient mice, few vessels were observed (mean 5.6 vessels/plug; SD ± 3.6 in wild-type, mean 6.6 vessels/plug; SD ± 5.1 in CCR6-deficient) (Fig. 10A). In Matrigel plugs containing 1,000 ng/ml CCL20, many vessels were observed after growth in wild-type mice (mean 23.8 vessels/plug; SD ± 22.2), whereas in CCR6-deficient mice significantly fewer vessels were present (mean 6.1 vessels/plug; SD ± 4.7). Importantly, in plugs from CCR6-deficient mice, the number of vessels in control plugs was comparable to that in the CCL20-containing plugs. These data therefore demonstrate that CCL20 is able to recruit CCR6-positive vessels. As a further control, CCL21 was included in Matrigel plugs. In C57BL/6 mice, vessel density was 1.3 vessels/plug (SD ± 2.1), whereas in CCR6-deficient mice the number of vessels was 8.7 vessels/plug (SD ± 3.4). This result demonstrates that vessel recruitment was specific to the CCL20/CCR6 interaction and not a general effect of supplying chemokines in Matrigel. The observation that CCL20 was able to promote vessel formation in the Matrigel plugs suggests tumor-derived CCL20 may be able to induce and/or enhance tumor angiogenesis.

5.7.2 Tumors in CCR6-deficient mice are smaller and less vascularized than tumors in wild-type mice

To investigate whether CCL20 influences tumor vascularization, B16/F10 tumor cells were used that express CCL20 (Fig 11.).

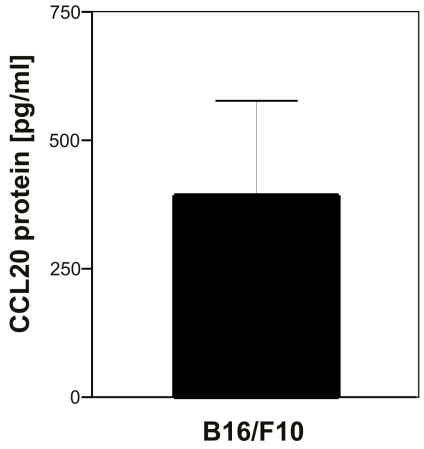

Fig. 11: B16/F10 tumor cells express CCL20. CCL20 protein expression in supernatants of B16/F10 tumor cells. Values are expressed in picograms per ml of supernatant.

B16/F10 tumor cells were subcutaneously injected into the hind limb of wild-type and CCR6-deficient C57BL/6 mice. Two weeks after injection of the cells, the vasculature inside the resulting tumors was imaged by flat panel volume computed tomography (fpVCT) to allow three-dimensional (3D) visualization of anatomical structures (Fig 10B). Analysis of differences in tumor and vessel growth between wild-type and CCR6-deficient mice revealed that subcutaneous B16/F10 tumors in wild-type mice recruited a dense network of blood vessels (Fig. 10B; white arrows), while tumors in CCR6-deficient mice showed dramatically fewer tumor-infiltrating vessels (Fig. 10B). Not only was the vascularization rate of tumors in wild-type mice increased, but also the number, size and diameter of the vessels were larger. At the end of the experiment tumor volume was analyzed, autopsies were performed and the tumors were excised and weighed (Fig. 10B). Tumors grown in CCR6-deficient mice had a significantly reduced volume and weight compared to tumors from wild-type mice. Furthermore, immunohistochemical

analysis of CD31-positive vessels in tumor sections revealed that there were fewer microvascular and macrovascular vessels inside the tumors from CCR6-deficient mice compared to the tumors from wild-type mice (Fig 10C). Together these data demonstrate that expression of the chemokine receptor CCR6 in the tumor microenvironment promotes tumor growth and is vital for efficient recruitment of vessels into the tumor.

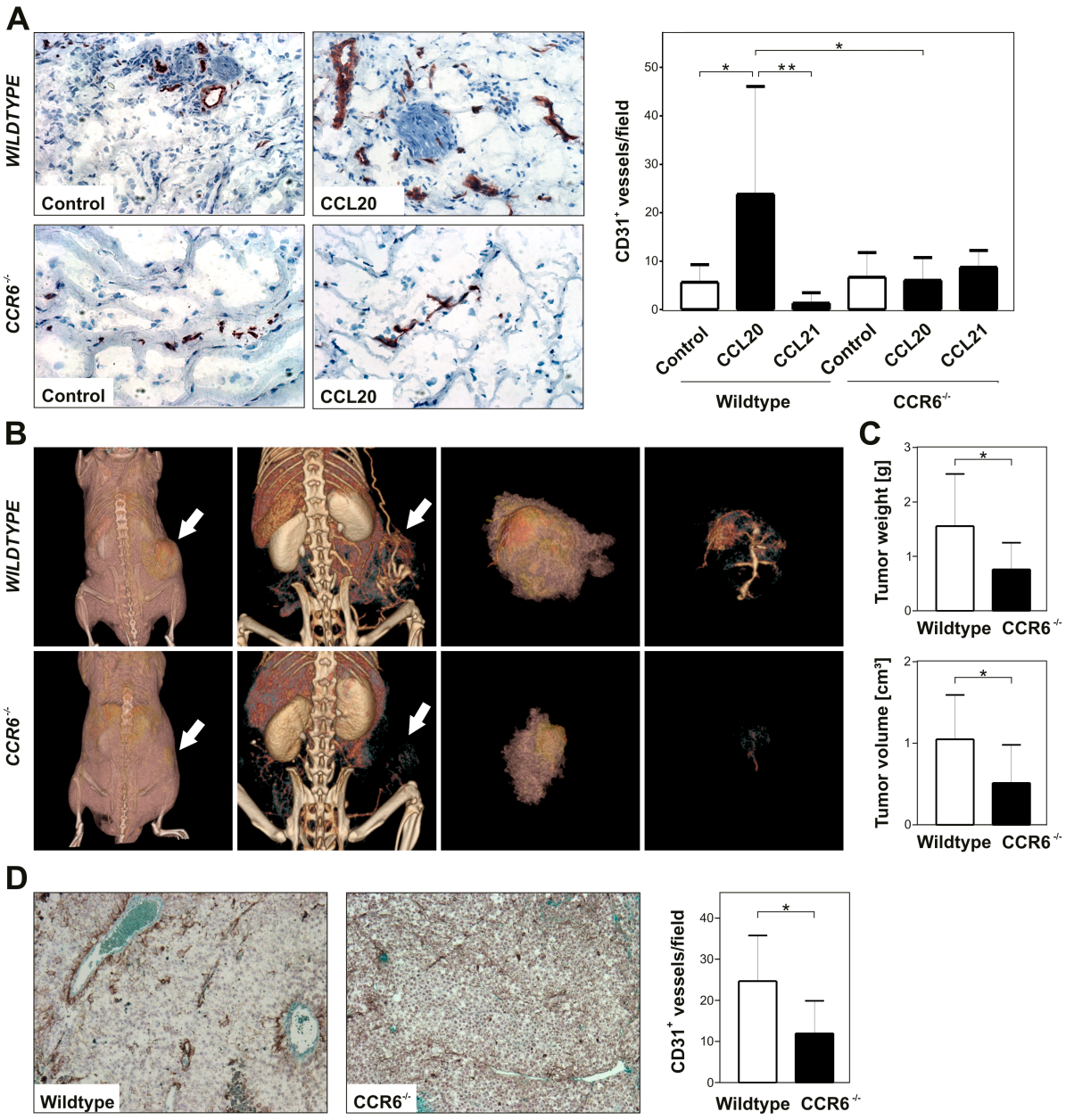

Fig. 10: CCL20/CCR6 signaling supports angiogenesis *in* vivo. (**A**) Cross-sections of Matrigel plugs removed 21 days after injection into C57BL/6 mice were stained with anti-CD31 antibodies (100x magnification). Representative pictures and the number of CD31-positive vessels per cross-section are shown and represent the mean ± SD of three independent experiments (*, P≤0.05; **, P≤0.01; Mann-Whitney U test). (**B**) Demonstration of contrast agent-containing tumor vessels and their distribution and bifurcations in the periphery and within a developing syngeneic CCL20-expressing B16/F10-tumor in C57BL/6 wildtype and C57BL/6-*CCR6*$^{-/-}$ mice by fpVCT scans. Representative results are shown and are indicated by white arrows. Tumor volume and weight of B16/F10-tumors in C57BL/6 wildtype and C57BL/6-*CCR6*$^{-/-}$ mice is measured in cubic centimeter and grams respectively and represent the mean ± SD of twelve independent tumors (*, P≤0.05; Mann-Whitney U test). (**C**) Analysis of vessel density of B16/F10 tumors of wildtype and CCR6-deficient mice by CD31 immunohistochemical stainings.

6 Discussion

In this study, a novel role of the chemokine CCL20 was investigated as a potential mediator in tumor-associated angiogenesis.

Are there further chemokines regulated by the MAPK signaling pathway?

The tumor microenvironment represents the site, where anti-tumoral and pro-tumoral factors, determine the course of tumor progression and prognosis of the disease. This study especially focused on the question, how tumors are able to modulate their microenvironment to facilitate their own growth.

Dysfunctional activation of EGFR and its downstream signaling pathways are known to be implicated in cancer. For instance, the EGF receptor is known to be overexpressed in wide variety of human solid tumors, including breast cancer, head-and-neck cancer, renal cancer, ovarian cancer, NSCLC, and colon cancer[117]. This overexpression results in intensified cellular signaling and increased activation of downstream signaling cascades, leading to more aggressive growth and an invasive phenotype[118].

Furthermore, mutational activation of the EGFR signaling dependent pathway MAPK is known to be implicated in many human cancers[25]. Increased MAPK signaling enhances processes crucial to tumor growth and progression, such as angiogenesis, tumor invasiveness, and metastatic spread[119].

In detail, oncogenic point mutations in the three human Ras genes, which are part of the MAPK pathway, have been detected in a majority of human cancers[120]. These mutational changes of Ras protein result in constitutive activation of Ras and of downstream signaling molecules[34].

In this work, the expressions of *CXCL14, CCL27*, *CXCL8* and *CCL20* were analyzed in HaCaT cell lines transfected with the activated H-RasV12 oncogene (Fig. 4) to get insights into the regulation of chemokine expression in keratinocyte-derived tumors. Results of the GTP-binding assay demonstrated increased Ras activity in cell lysates of H-RasV12-transfected cell lines compared with untransfected cells (Fig 4A).

Examining chemokine expression by qPCR, it was observed that untransfected HaCaT cells showed different chemokine mRNA levels in comparison to transfected HaCaT cells

(Fig. 4). This study demonstrates that activation of Ras down-regulates a set of chemokines (*CXCL14* and *CCL27*), while it increases *CCL20* and *CXCL8* gene expression in H-RasV12 transfected HaCaT keratinocytes.

CXCL14, which is a CXC-type chemokine with unknown receptor selectivity[121], was identified by Hromas *et al.* by translating expressed sequence tags (ESTs) derived from breast and kidney carcinoma libraries[122]. CXCL14 was found to be expressed ubiquitously in RNA from normal tissue extracts, foremost in those of epithelial origin such as the skin and the gastrointestinal tract[121]. The observation of this study, that CXCL14 expression is down-regulated in a Ras-dependent manner (Fig. 4B), corresponds to the finding of Ozawa *et al.*, who demonstrated the down regulation of CXCL14 in HNSCC cells after treatment with EGF[123]. Ozawa *et al.* also showed that EGF down regulated CXCL14 expression through the MEK–ERK pathway and the retrieval of CXCL14 expression by treatment with gefitinib, an inhibitor against the tyrosine-kinase domain of EGFR[123]. Additionally, oral application of gefitinib increased CXCL14 expression specifically in tumor tissue of xenografts (transplantation of cells or tissue between different species) of three HNSCC cell lines (HSC-2, HSC-3, and HSC-4) in female athymic nude mice[123].

In addition to CXCL14, another chemokine, namely CCL27, showed a Ras-dependent regulation in this study (Fig. 4C). Correlating with the results of this study, Pivarcsi *et al.* could demonstrate in a recent publication that human keratinocyte-derived skin tumors may evade T cell-mediated antitumor immune responses by down-regulating the expression of CCL27 through the activation of epidermal growth factor receptor (EGFR)-Ras-MAPK-signaling pathways[104].

Furthermore, it has been shown that activation of Ras is not only involved in the down regulation of chemokine expression, but also upregulates chemokine production. Sparmann *et al.* showed that activation of Ras in cervical cancer cells induces the expression of the proinflammatory chemokine CXCL8. The same effect could be shown here. CXCL8 plays an important role in tumor growth and angiogenesis[103]. Altogether, the studies of Ozawa *et al.*, Pivarcsi *et al.* and Sperman *et al.* confirm the oncogenic Ras/keratinocyte-model chosen in this study to demonstrate the involvement of the MAPK signaling pathway in chemokine expression. The Ras-dependent differential chemokine expression leads to an altered chemokine expression profile, suggesting a chemokine driven modulation of the tumor microenvironment.

One other chemokine gene expression was induced due to an activated MAPK signaling

pathway – the expression of the chemokine CCL20 (Fig. 4D, 5, 7A; Tab. 4). Interestingly, no studies, to current knowledge, have evaluated the direct effect of Ras on the expression of CCL20 in keratinocytes. *In vitro*, stimulation of the EGFR–Ras signaling pathway through the dominant-active form of the Ras oncogene (H-RasV12) increased, whereas the EGFR tyrosine kinase inhibitor erlotinib suppressed, CCL20 mRNA and protein production in immortalized keratinocytes (Fig. 5). Furthermore, expression of CCL20 co-localized to areas of ERK activation in immunohistochemical analyses of human breast cancer-, melanoma- and squamous cell carcinoma- tissues (Fig. 7A). This finding was verified by immunohistochemical stainings of tumor tissue microarrays containing 121 tissues of breast cancer and HNSCC patients for CCL20 and pERK. Analysis of data showed a highly significant correlation between elevated CCL20 expression and activated ERK (Tab. 4), suggesting an EGFR/Ras/ERK-dependent expression of CCL20.

Activation of CCL20 expression via ERK was shown to be presumably orchestrated by the epithelium-specific Ets nuclear factor ESE-1. Kwon *et al.* identified a 5' regulatory element of the human CCL20 promoter by scanning mutagenesis and demonstrated that ESE-1 is an important co-regulator of CCL20 gene expression in Caco-2 colonic epithelial cells[124]. Specific mutations in this 5' sequence significantly reduced CCL20 gene expression[124].

Ets-like binding elements have previously been shown to be involved in the regulation of other chemokine genes, including CXCL4, CXCL7, CCL5, CCL3, and CCL7[125,126,127,128,129]. The *CXCL4* promoter was found to be transactivated by the ubiquitously expressed factor Ets-1, whereas PU.1, an Ets factor restricted primarily to cells of the immune system, regulated *CXCL7* gene expression. For CCL5, CCL3, and CCL7 the specific Ets factor regulating gene expression was not identified.

From regulatory to expressional level: Do tumors express EGFR/Ras-regulated CCL20 and what are the physiological and clinical effects of tumor-derived CCL20 expression?

The activation of the EGFR/Ras/Raf/MEK/Erk signaling pathway is implicated in a wide variety of tumors. Based on the observation that *CCL20* gene is highly expressed in human immortalized keratinocytes and is upregulated by activated oncogenic Ras, CCL20 expression was determined in a multitude of tumor cell lines (Fig. 6). In this study elevated

expression of CCL20 was found in cancer cell lines of melanoma, breast cancer and squamous cell carcinoma on the mRNA level, in comparison to their benign precursor cells (Fig. 6A-C). CCL20 protein expression was also discovered in cell lines of these tumors (Fig. 6D). This is in line with the observation that CCL20 is expressed by various human cancer entities, such as leukemia, lymphoma, melanoma, hepatocellular carcinoma, prostate cancer, colorectal adenocarcinoma and lung and oral squamous cell carcinoma[130,131,132,133]. Furthermore, tumor biopsies taken from patients suffering from different cancers were analyzed by qPCR in this study. *CCL20* expression increased in the course of tumor progression, as expression of *CCL20* was significantly higher in metastases of breast cancer and melanoma in comparison to normal breast tissue or primary melanocytes (Fig. 6E). Additionally, biopsies acquired from HNSCC patients showed a significant higher *CCL20* expression in primary tumors compared to normal mucosa.

Similarly to the findings of elevated CCL20 expression in malignant cells, Bordoni *et al.* reported CXCL1 mRNA to be constitutively expressed in nevocytes and melanoma, whereas CXCL1 expression was not detectable in primary melanocytes[134]. The findings demonstrate a change of the chemokine expression profile during tumor progression. The observation that tumors express the chemokine CCL20 and that tumors of higher stages express higher levels of CCL20, gave rise to the assumption that CCL20 is involved in tumor progression. To verify this thesis, comprehensive immunohistochemical stainings for CCL20 in tumor tissue microarrays composed of 334 tumors of breast cancer, colon carcinoma and HNSCC, were compared to patients' data. And indeed the analysis showed that a high pT- or pN-category of the 334 investigated tumors of breast cancer, colon carcinoma and HNSCC significantly correlates with elevated CCL20 expression levels (Tab. 5).

Similarly, in pancreatic cancer tissues the CCL20 transcript was detected in moderate to high levels[135] and expression of the CCL20 protein was observed in cancer cells within the pancreatic tumor mass[136]. In accordance with these studies, Rubie *et al.* have observed a significant up-regulation of CCL20 mRNA and protein expression in pancreatic cancer. Interestingly, comparing several clinicopathological factors to CCL20 mRNA and protein expression levels Rubie *et al.* found a significant correlation with advanced T-category pointing to a role for CCL20 and CCR6 in progression of pancreatic cancer[137]. These data suggest that tumors expressing high levels of CCL20 have a more aggressive phenotype.

Next, to investigate clinical effects of tumor-derived CCL20, follow-up data of 40 breast cancer patients were compared to CCL20 expression in the tumors. The analysis revealed a correlation of elevated CCL20 expression in primary tumors with a decreased cumulative survival of breast cancer patients (Fig 7C). Since elevated CCL20 expression in tumors were shown to correlate with advanced pT- and pN-category, the lowered cumulative survival of breast cancer patients could be a result of CCL20-dependent increased tumor growth and metastasis.

Consequently, this study demonstrated the expression of CCL20 in a multitude of tumors and it was shown that high CCL20 expression levels promote tumor progression and growth and correspond to negative effects on the survival of breast cancer patients. These results raise the question for the underlying mechanism of CCL20-dependent tumor progression and the role of CCL20 in the tumor microenvironment needed to be addressed.

Pro- versus anti-tumor effects: A novel role for CCL20 in tumor biology?

CCL20 was initially designated as liver and activation regulated chemokine (LARC) because its constitutive expression was first observed in the liver. Alternative names are macrophage inflammatory protein-3a (MIP-3a) and Exodus-1[138]. CCL20 is a 9-kDa CC-type chemokine[139] and the constitutive expression of CCL20 was also shown in mucosa-associated lymphatic tissue (MALT), other lymphatic tissues and lung tissue[138]. CCL20 expression has additionally been demonstrated in macrophages, dendritic cells, B- and T-lymphocytes, eosinophilic granulocytes as well as normal tissue of the colon, pancreas, prostate, uterine cervix and skin[138]. Interestingly, in contrast to most of the chemokine family members, CCL20 specifically binds only to one chemokine receptor, CCR6[140,141]. CCR6 has been demonstrated to be expressed on immature dendritic cells (DCs), memory T lymphocytes (T cells) and naive B lymphocytes (B cells), suggesting that CCR6 plays an important role in adaptive immunity[141]. This notion is further exemplified by CCR6/CCL20-dependent immature DC migration[141] to peripheral organs, especially the epidermis, where CCL20 is expressed by keratinocytes and venular endothelial cells[142]. These immature DCs, so called Langerhans cells (LCs), a $CD1a^+$ subpopulation of dendritic cells, enter the skin to screen the epidermis constitutively[142] against invasive pathogens[141]. However, after dendritic cell maturation, a loss of CCR6 surface expression

has been reported[143]. Subsequently, mature dendritic cells are recruited to the lymph nodes by expression of CCR7[144]. In the lymph nodes, mature dendritic cells are able to activate $CD8^+$ T-cells[145]. Overexpression of CCL20 in tumors or its injection into tumors has confirmed the recruitment of CCR6-positive immature dendritic cells to the tumor site[146]. The current data suggest a pivotal role for CCL20 in immune surveillance and defense. This immuno-modulatory effect of CCL20 was instrumental in postulating an anti-tumor role for the chemokine.

However, the role of tumor-associated immune cells in tumor progression has remained ambiguous. It is contradictory that tumor cells would secrete chemokines, which would increase an immune response against themselves. Balkwill *et al.* and others described neoplastic tissue as a Darwinian microenvironment that selects for the type and extent of inflammation, which is promoting tumor growth and progression[147]. Recently, dendritic cells, which were recruited to sites of melanoma and colorectal cancer, were shown to exhibit a more immature than mature phenotype. In addition, melanoma-conditioned DCs exhibited an increased adhesion capacity to a melanoma cell line *in vitro* by expression of the adhesion molecules E-cadherin and CD15[148]. Furthermore, DCs treated with conditioned medium from melanoma cell lines did not migrate in response to the chemokine CCL21[148], which is expressed by lymphatic vessels and lymph nodes and binds to its receptor CCR7. As a result, DC motility could be severely diminished by tumor cells. Overexpression of CCL20 in tumors or its injection into tumors results in the recruitment of CCR6-positive immature dendritic cells into the tumor[146]. However, tumors derived from B16 melanoma cells with high CCL20 expression only regressed after an additional challenge to the tumor with deoxycytidyl-deoxyguanosine (CpG) injections[146]. CpG-oligonucleotides mimic the immunostimulatory activity of bacterial DNA and are recognized by the Toll-like receptor-9 of DCs[149,150]. These data suggest that recruitment of immature dendritic cells by CCL20 to the tumor is by itself insufficient for a tumor immune response, and that dendritic cell maturation is required in addition. A further indication for a pro-tumor role of CCL20 was given by Kleeff *et al.* They observed that tumor-associated macrophages (TAMs) abundantly expressed CCL20 and promoted growth and migration of two $CCR6^+$ pancreatic cancer cell lines[135], suggesting an additional autocrine stimulation of CCL20-expresssing tumor cells.

Because of this ambivalent picture generated by the current known pro- and anti-tumor effects of CCL20, the role of this chemokine in the tumor microenvironment was investigated. Since CCL20 attracts $CCR6^+$ cells, the tumor microenvironment was

analyzed for further CCR6-positive cells, which are able to respond to the chemokine. For the first time, in this study the specific receptor of CCL20, namely CCR6, was found to be expressed on the surface of human dermal microvascular blood endothelial cells (BECs) and human dermal microvascular lymphatic endothelial cells (LECs) (Fig. 8A-B). These cells line all dermal microvascular vessels. Additionally, immunofluorescent stainings revealed $CCR6^+$ vessels in the outer boundary of tumors (Fig. 8C). As tumors are dependent on the supply with oxygen and nutrients delivered by vessels, it was postulated that tumors may promote their own growth by CCL20-dependent attraction of $CCR6^+$ endothelial cells, suggesting a role for CCL20 in angiogenesis. And indeed, ligand-receptor interaction was shown to be functional in *in vitro* chemotaxis assays (Fig. 9A), where $CCR6^+$ endothelial cells migrated in the direction of a CCL20 gradient. This phenomenon could not be observed when the cells were exposed to the irrelevant chemokine CCL21, or when the receptor CCR6 was blocked with an antibody against CCR6. Similarly, Salcedo *et al.* demonstrated angiogenic potential of endothelial cells towards chemokines by showing response of HUVECs and HMECs towards the chemokine CCL2 in micro-Boyden chambers[55]. Blocking of CCL2 with a polyclonal antibody specifically inhibited the chemotactic response[55].

Additionally, in this study treatment of BECs with CCL20 enhanced their natural ability to form tube-like structures in *in vitro* tube formation assays (Fig. 9F), also proving a role for CCL20 in the formation of vessels. The ability of chemokines to enhance formation of tubes was shown before by Wang *et al.* They demonstrated the potential of the chemokine CXCL1, which was released from prostate carcinoma cells, to elevate microvascular endothelial cell migration and tube formation *in vitro*[151].

To validate these findings *in vivo* and provide proof of principle, advantage was taken of a CCR6-deficient mouse strain and the role of CCL20 was analyzed in two different models.

First, results were verified by *in vivo* Matrigel plug assays (Fig. 10A). The Matrigel plug assay is a suitable assay to mimic the influence of a chemokine-expressing tumor to its microenvironment as all other influences of a tumor are excluded. It was observed that CCL20 was able to promote vessel formation in CCL20 containing Matrigel plugs of wild-type mice, whereas this effect was significantly diminished in CCR6 knock out mice. These findings suggested a pivotal role for CCL20 in tumor-associated angiogenesis. Likewise, Salcedo *et al.* investigated the angiogenic effect of CCL2 also using an *in vivo* Matrigel plug assay. Mice were injected with Matrigel alone or with CCL2 containing

Matrigel subcutaneously in the flank. Histologic examination of the Matrigel plugs indicated a significant angiogenic effect induced by CCL2 in contrast to Matrigel alone[55].
Finally, this study was able to demonstrate the CCL20/CCR6-dependent vascularization of CCL20 expressing tumors in a murine syngeneic tumor model. Wild-type mice and CCR6 knock out mice were treated with CCL20-expressing B16/F10 melanoma cells and analyzed by means of fpVCT and immunohistochemical stainings (Fig. 10B-C). B16/F10 melanoma of wild-type mice were significantly heavier and larger in size, and were much more vascularized than melanoma of CCR6 knock out mice verifying the CCL20-dependet vessel attraction into the tumor.

In summary, the results of the performed study suggest a novel role for CCL20 in angiogenesis. To date a role for CCL20 in endothelial cell recruitment and angiogenesis has not been described. In CCL20-expressing tumors, more vessels were present when grown in a CCR6-positive background. Moreover, CCL20-expressing tumors were more advanced and, in the case of breast cancer, patients had a worse survival prognosis than patients whose primary tumors showed only low CCL20 expression. These findings present strong evidence that the tumor-promoting effects of CCL20, for example through the enhancement of angiogenesis, are more important for tumor progression than any adverse effects on tumor growth caused by CCL20-mediated recruitment of immature dendritic cells. It is conceivable that maturation of dendritic cells, a vital process for enhancing the immune response through CCL20, is repressed through as yet unknown tumor-derived factors.

CCL20 was demonstrated to be a novel angiogenic chemokine that is expressed in tumors via activation of the EGFR/Ras signal transduction pathway. The CCL20 receptor CCR6 therefore represents a promising target for anti-cancer therapy. Specifically, blocking the activity of CCR6 in the microenvironment of the tumor might inhibit tumor neo-angiogenesis and thereby enhance conventional anti-tumor therapies.

7 References

1 *Krebs in Deutschland 2005/2006. Häufigkeiten und Trends.* 7th edn, (Robert Koch-Institute (Hrsg) und die Gesellschaft der epidermiologischen Krebsregister in Deutschland e.V. (Hrsg). 2010).

2 Cummins, D. L. *et al.* Cutaneous malignant melanoma. *Mayo Clin Proc* **81**, 500-507 (2006).

3 Cascinelli, N. *et al.* What is the most promising strategy for the treatment of metastasizing melanoma? *Exp Dermatol* **9**, 439-451 (2000).

4 Streit, M. & Detmar, M. Angiogenesis, lymphangiogenesis, and melanoma metastasis. *Oncogene* **22**, 3172-3179, (2003).

5 Keshtgar, M., Davidson, T., Pigott, K., Falzon, M. & Jones, A. Current status and advances in management of early breast cancer. *Int J Surg* **8**, 199-202, (2010).

6 Gil, Z. & Fliss, D. M. Contemporary management of head and neck cancers. *Isr Med Assoc J* **11**, 296-300 (2009).

7 Wilkes, G. & Hartshorn, K. Colon, rectal, and anal cancers. *Semin Oncol Nurs* **25**, 32-47, (2009).

8 Weidner, N., Semple, J. P., Welch, W. R. & Folkman, J. Tumor angiogenesis and metastasis--correlation in invasive breast carcinoma. *N Engl J Med* **324**, 1-8, (1991).

9 Weidner, N., Carroll, P. R., Flax, J., Blumenfeld, W. & Folkman, J. Tumor angiogenesis correlates with metastasis in invasive prostate carcinoma. *Am J Pathol* **143**, 401-409 (1993).

10 Brawer, M. K. Quantitative microvessel density. A staging and prognostic marker

for human prostatic carcinoma. *Cancer* **78**, 345-349, (1996).

11 Yamazaki, K. *et al.* Tumor angiogenesis in human lung adenocarcinoma. *Cancer* **74**, 2245-2250 (1994).

12 Angeletti, C. A. *et al.* Prognostic significance of tumoral angiogenesis in completely resected late stage lung carcinoma (stage IIIA-N2). Impact of adjuvant therapies in a subset of patients at high risk of recurrence. *Cancer* **78**, 409-415, (1996).

13 Maeda, K. *et al.* Tumor angiogenesis as a predictor of recurrence in gastric carcinoma. *J Clin Oncol* **13**, 477-481 (1995).

14 Wiggins, D. L., Granai, C. O., Steinhoff, M. M. & Calabresi, P. Tumor angiogenesis as a prognostic factor in cervical carcinoma. *Gynecol Oncol* **56**, 353-356, (1995).

15 Hollingsworth, H. C., Kohn, E. C., Steinberg, S. M., Rothenberg, M. L. & Merino, M. J. Tumor angiogenesis in advanced stage ovarian carcinoma. *Am J Pathol* **147**, 33-41 (1995).

16 Kashani-Sabet, M., Sagebiel, R. W., Ferreira, C. M., Nosrati, M. & Miller, J. R., 3rd. Tumor vascularity in the prognostic assessment of primary cutaneous melanoma. *J Clin Oncol* **20**, 1826-1831 (2002).

17 Takebayashi, Y., Aklyama, S., Yamada, K., Akiba, S. & Aikou, T. Angiogenesis as an unfavorable prognostic factor in human colorectal carcinoma. *Cancer* **78**, 226-231, (1996).

18 Onogawa, S. *et al.* Expression of VEGF-C and VEGF-D at the invasive edge correlates with lymph node metastasis and prognosis of patients with colorectal carcinoma. *Cancer Sci* **95**, 32-39 (2004).

19 Saad, R. S. *et al.* Lymphatic microvessel density as prognostic marker in colorectal cancer. *Mod Pathol* **19**, 1317-1323, (2006).

[20] Gasparini, G. *et al.* Intratumoral microvessel density and p53 protein: correlation with metastasis in head-and-neck squamous-cell carcinoma. *Int J Cancer* **55**, 739-744 (1993).

[21] Carmeliet, P. & Jain, R. K. Angiogenesis in cancer and other diseases. *Nature* **407**, 249-257, (2000).

[22] Hoshino, R. *et al.* Constitutive activation of the 41-/43-kDa mitogen-activated protein kinase signaling pathway in human tumors. *Oncogene* **18**, 813-822, (1999).

[23] Bier, H., Hoffmann, T., Haas, I. & van Lierop, A. Anti-(epidermal growth factor) receptor monoclonal antibodies for the induction of antibody-dependent cell-mediated cytotoxicity against squamous cell carcinoma lines of the head and neck. *Cancer Immunol Immunother* **46**, 167-173 (1998).

[24] Miettinen, P. J. *et al.* Epithelial immaturity and multiorgan failure in mice lacking epidermal growth factor receptor. *Nature* **376**, 337-341, (1995).

[25] Ferguson, K. M. *et al.* EGF activates its receptor by removing interactions that autoinhibit ectodomain dimerization. *Mol Cell* **11**, 507-517, (2003).

[26] Yarden, Y. The EGFR family and its ligands in human cancer. signalling mechanisms and therapeutic opportunities. *Eur J Cancer* **37 Suppl 4**, S3-8, (2001).

[27] Herbst, R. S. Review of epidermal growth factor receptor biology. *Int J Radiat Oncol Biol Phys* **59**, 21-26, (2004).

[28] Salomon, D. S., Brandt, R., Ciardiello, F. & Normanno, N. Epidermal growth factor-related peptides and their receptors in human malignancies. *Crit Rev Oncol Hematol* **19**, 183-232, (1995).

[29] Toyoda, H., Komurasaki, T., Ikeda, Y., Yoshimoto, M. & Morimoto, S. Molecular cloning of mouse epiregulin, a novel epidermal growth factor-related protein, expressed in the early stage of development. *FEBS Lett* **377**, 403-407, (1995).

[30] Mendelsohn, J. & Baselga, J. Epidermal growth factor receptor targeting in cancer. *Semin Oncol* **33**, 369-385, (2006).

[31] Nishida, E. & Gotoh, Y. The MAP kinase cascade is essential for diverse signal transduction pathways. *Trends Biochem Sci* **18**, 128-131, (1993).

[32] Cobb, M. H. & Goldsmith, E. J. How MAP kinases are regulated. *J Biol Chem* **270**, 14843-14846 (1995).

[33] Seger, R. & Krebs, E. G. The MAPK signaling cascade. *FASEB J* **9**, 726-735 (1995).

[34] Pollard, T. D., Earnshaw, W. C. & Lippincott-Schwartz, J. *Cell biology*. 2nd edn, (Saunders/Elsevier, 2008).

[35] Gray-Schopfer, V., Wellbrock, C. & Marais, R. Melanoma biology and new targeted therapy. *Nature* **445**, 851-857, (2007).

[36] Davis, R. J. The mitogen-activated protein kinase signal transduction pathway. *J Biol Chem* **268**, 14553-14556 (1993).

[37] Bos, J. L. ras oncogenes in human cancer: a review. *Cancer Res* **49**, 4682-4689 (1989).

[38] Barbacid, M. ras genes. *Annu Rev Biochem* **56**, 779-827, (1987).

[39] Alison, M. R. (John Wiley & Sons, 2007).

[40] Yao, M., Shuin, T., Misaki, H. & Kubota, Y. Enhanced expression of c-myc and epidermal growth factor receptor (C-erbB-1) genes in primary human renal cancer. *Cancer Res* **48**, 6753-6757 (1988).

[41] Shimizu, K. *et al.* Three human transforming genes are related to the viral ras oncogenes. *Proc Natl Acad Sci U S A* **80**, 2112-2116 (1983).

[42] Bos, J. L. The ras gene family and human carcinogenesis. *Mutat Res* **195**, 255-271 (1988).

[43] Sini, P. *et al.* The antitumor and antiangiogenic activity of vascular endothelial growth factor receptor inhibition is potentiated by ErbB1 blockade. *Clin Cancer Res* **11**, 4521-4532, (2005).

[44] Goldman, C. K. *et al.* Epidermal growth factor stimulates vascular endothelial growth factor production by human malignant glioma cells: a model of glioblastoma multiforme pathophysiology. *Mol Biol Cell* **4**, 121-133 (1993).

[45] Bianco, R. *et al.* Combined targeting of epidermal growth factor receptor and MDM2 by gefitinib and antisense MDM2 cooperatively inhibit hormone-independent prostate cancer. *Clin Cancer Res* **10**, 4858-4864, (2004).

[46] Bruns, C. J. *et al.* Blockade of the epidermal growth factor receptor signaling by a novel tyrosine kinase inhibitor leads to apoptosis of endothelial cells and therapy of human pancreatic carcinoma. *Cancer Res* **60**, 2926-2935 (2000).

[47] Solorzano, C. C. *et al.* Optimization for the blockade of epidermal growth factor receptor signaling for therapy of human pancreatic carcinoma. *Clin Cancer Res* **7**, 2563-2572 (2001).

[48] Dieter Marmé, N. F. (Springer, Berlin Heidelberg, 2008).

[49] Conway, E. M., Collen, D. & Carmeliet, P. Molecular mechanisms of blood vessel growth. *Cardiovasc Res* **49**, 507-521, (2001).

[50] Auerbach, R., Kubai, L. & Sidky, Y. Angiogenesis induction by tumors, embryonic tissues, and lymphocytes. *Cancer Res* **36**, 3435-3440 (1976).

[51] Folkman, J. Angiogenesis in cancer, vascular, rheumatoid and other disease. *Nat Med* **1**, 27-31 (1995).

[52] Folkman, J. & Shing, Y. Angiogenesis. *J Biol Chem* **267**, 10931-10934 (1992).

[53] Lippert. *Lehrbuch Anatomie*. 7th edn, (Elsevier, 2006).

[54] Bernardini, G. *et al.* Analysis of the role of chemokines in angiogenesis. *J Immunol Methods* **273**, 83-101, (2003).

[55] Salcedo, R. *et al.* Human endothelial cells express CCR2 and respond to MCP-1: direct role of MCP-1 in angiogenesis and tumor progression. *Blood* **96**, 34-40 (2000).

[56] Baker, C. H. *et al.* Blockade of epidermal growth factor receptor signaling on tumor cells and tumor-associated endothelial cells for therapy of human carcinomas. *Am J Pathol* **161**, 929-938 (2002).

[57] Hirata, A. *et al.* ZD1839 (Iressa) induces antiangiogenic effects through inhibition of epidermal growth factor receptor tyrosine kinase. *Cancer Res* **62**, 2554-2560 (2002).

[58] Neufeld, G., Cohen, T., Gengrinovitch, S. & Poltorak, Z. Vascular endothelial growth factor (VEGF) and its receptors. *FASEB J* **13**, 9-22 (1999).

[59] Sumpio, B. E., Riley, J. T. & Dardik, A. Cells in focus: endothelial cell. *Int J*

Biochem Cell Biol **34**, 1508-1512, (2002).

60 Tsai, H. M. Shear stress and von Willebrand factor in health and disease. *Semin Thromb Hemost* **29**, 479-488, (2003).

61 Jain, R. K. Molecular regulation of vessel maturation. *Nat Med* **9**, 685-693, (2003).

62 Iivanainen, E., Kahari, V. M., Heino, J. & Elenius, K. Endothelial cell-matrix interactions. *Microsc Res Tech* **60**, 13-22, (2003).

63 Genis, L., Galvez, B. G., Gonzalo, P. & Arroyo, A. G. MT1-MMP: universal or particular player in angiogenesis? *Cancer Metastasis Rev* **25**, 77-86, (2006).

64 Karamysheva, A. F. Mechanisms of angiogenesis. *Biochemistry (Mosc)* **73**, 751-762, (2008).

65 Kume, T. Novel insights into the differential functions of Notch ligands in vascular formation. *J Angiogenes Res* **1**, 8, (2009).

66 Gerhardt, H. *et al.* VEGF guides angiogenic sprouting utilizing endothelial tip cell filopodia. *J Cell Biol* **161**, 1163-1177, (2003).

67 Bergers, G. & Song, S. The role of pericytes in blood-vessel formation and maintenance. *Neuro Oncol* **7**, 452-464, (2005).

68 Enge, M. *et al.* Endothelium-specific platelet-derived growth factor-B ablation mimics diabetic retinopathy. *EMBO J* **21**, 4307-4316 (2002).

69 Hippe, A., Homey, B. & Mueller-Homey, A. Chemokines. *Recent Results Cancer Res* **180**, 35-50, (2010).

[70] Tannock, I. F. & Hayashi, S. The proliferation of capillary endothelial cells. *Cancer Res* **32**, 77-82 (1972).

[71] Engerman, R. L., Pfaffenbach, D. & Davis, M. D. Cell turnover of capillaries. *Lab Invest* **17**, 738-743 (1967).

[72] Leibovich, S. J. & Wiseman, D. M. Macrophages, wound repair and angiogenesis. *Prog Clin Biol Res* **266**, 131-145 (1988).

[73] Muller, A. *et al.* Involvement of chemokine receptors in breast cancer metastasis. *Nature* **410**, 50-56, (2001).

[74] Zlotnik, A. & Yoshie, O. Chemokines: a new classification system and their role in immunity. *Immunity* **12**, 121-127, (2000).

[75] Thelen, M. Dancing to the tune of chemokines. *Nat Immunol* **2**, 129-134, (2001).

[76] Sallusto, F., Lanzavecchia, A. & Mackay, C. R. Chemokines and chemokine receptors in T-cell priming and Th1/Th2-mediated responses. *Immunol Today* **19**, 568-574, (1998).

[77] Horuk, R. Chemokine receptors. *Cytokine Growth Factor Rev* **12**, 313-335, (2001).

[78] Zlotnik, A., Yoshie, O. & Nomiyama, H. The chemokine and chemokine receptor superfamilies and their molecular evolution. *Genome Biol* **7**, 243, (2006).

[79] Lazennec, G. & Richmond, A. Chemokines and chemokine receptors: new insights into cancer-related inflammation. *Trends Mol Med* **16**, 133-144, (2010).

[80] Power, C. A. *et al.* Cloning and characterization of a specific receptor for the novel CC chemokine MIP-3alpha from lung dendritic cells. *J Exp Med* **186**, 825-835

(1997).

81 Liao, F. *et al.* STRL22 is a receptor for the CC chemokine MIP-3alpha. *Biochem Biophys Res Commun* **236**, 212-217, (1997).

82 Raman, D., Baugher, P. J., Thu, Y. M. & Richmond, A. Role of chemokines in tumor growth. *Cancer Lett* **256**, 137-165, (2007).

83 Strieter, R. M. *et al.* The functional role of the ELR motif in CXC chemokine-mediated angiogenesis. *J Biol Chem* **270**, 27348-27357 (1995).

84 Addison, C. L. *et al.* The CXC chemokine receptor 2, CXCR2, is the putative receptor for ELR+ CXC chemokine-induced angiogenic activity. *J Immunol* **165**, 5269-5277 (2000).

85 Murdoch, C., Monk, P. N. & Finn, A. Cxc chemokine receptor expression on human endothelial cells. *Cytokine* **11**, 704-712, (1999).

86 Heidemann, J. *et al.* Angiogenic effects of interleukin 8 (CXCL8) in human intestinal microvascular endothelial cells are mediated by CXCR2. *J Biol Chem* **278**, 8508-8515, (2003).

87 Goede, V., Brogelli, L., Ziche, M. & Augustin, H. G. Induction of inflammatory angiogenesis by monocyte chemoattractant protein-1. *Int J Cancer* **82**, 765-770, (1999).

88 Adler, E. P., Lemken, C. A., Katchen, N. S. & Kurt, R. A. A dual role for tumor-derived chemokine RANTES (CCL5). *Immunol Lett* **90**, 187-194, (2003).

89 Son, K. N., Hwang, J., Kwon, B. S. & Kim, J. Human CC chemokine CCL23 enhances expression of matrix metalloproteinase-2 and invasion of vascular endothelial cells. *Biochem Biophys Res Commun* **340**, 498-504, (2006).

[90] Owen, M. R., Alarcon, T., Maini, P. K. & Byrne, H. M. Angiogenesis and vascular remodelling in normal and cancerous tissues. *J Math Biol* **58**, 689-721, (2009).

[91] Luan, J. *et al.* Mechanism and biological significance of constitutive expression of MGSA/GRO chemokines in malignant melanoma tumor progression. *J Leukoc Biol* **62**, 588-597 (1997).

[92] Owen, J. D. *et al.* Enhanced tumor-forming capacity for immortalized melanocytes expressing melanoma growth stimulatory activity/growth-regulated cytokine beta and gamma proteins. *Int J Cancer* **73**, 94-103, (1997).

[93] Chavey, C. *et al.* Oestrogen receptor negative breast cancers exhibit high cytokine content. *Breast Cancer Res* **9**, R15, (2007).

[94] Ueno, T. *et al.* Significance of macrophage chemoattractant protein-1 in macrophage recruitment, angiogenesis, and survival in human breast cancer. *Clin Cancer Res* **6**, 3282-3289 (2000).

[95] Saji, H. *et al.* Significant correlation of monocyte chemoattractant protein-1 expression with neovascularization and progression of breast carcinoma. *Cancer* **92**, 1085-1091, (2001).

[96] Brouty-Boye, D. & Zetter, B. R. Inhibition of cell motility by interferon. *Science* **208**, 516-518 (1980).

[97] Folkman, J. Angiogenesis and apoptosis. *Semin Cancer Biol* **13**, 159-167, (2003).

[98] Belperio, J. A. *et al.* CXC chemokines in angiogenesis. *J Leukoc Biol* **68**, 1-8 (2000).

[99] Keane, M. P., Belperio, J. A., Xue, Y. Y., Burdick, M. D. & Strieter, R. M. Depletion of CXCR2 inhibits tumor growth and angiogenesis in a murine model of lung

cancer. *J Immunol* **172**, 2853-2860 (2004).

[100] Shellenberger, T. D. *et al.* BRAK/CXCL14 is a potent inhibitor of angiogenesis and a chemotactic factor for immature dendritic cells. *Cancer Res* **64**, 8262-8270, (2004).

[101] Struyf, S., Burdick, M. D., Proost, P., Van Damme, J. & Strieter, R. M. Platelets release CXCL4L1, a nonallelic variant of the chemokine platelet factor-4/CXCL4 and potent inhibitor of angiogenesis. *Circ Res* **95**, 855-857, (2004).

[102] Lasagni, L. *et al.* An alternatively spliced variant of CXCR3 mediates the inhibition of endothelial cell growth induced by IP-10, Mig, and I-TAC, and acts as functional receptor for platelet factor 4. *J Exp Med* **197**, 1537-1549, (2003).

[103] Sparmann, A. & Bar-Sagi, D. Ras-induced interleukin-8 expression plays a critical role in tumor growth and angiogenesis. *Cancer Cell* **6**, 447-458, (2004).

[104] Pivarcsi, A. *et al.* Tumor immune escape by the loss of homeostatic chemokine expression. *Proc Natl Acad Sci U S A* **104**, 19055-19060, (2007).

[105] Phillips, R. J. *et al.* Epidermal growth factor and hypoxia-induced expression of CXC chemokine receptor 4 on non-small cell lung cancer cells is regulated by the phosphatidylinositol 3-kinase/PTEN/AKT/mammalian target of rapamycin signaling pathway and activation of hypoxia inducible factor-1alpha. *J Biol Chem* **280**, 22473-22481, (2005).

[106] Cook, D. N. *et al.* CCR6 mediates dendritic cell localization, lymphocyte homeostasis, and immune responses in mucosal tissue. *Immunity* **12**, 495-503, (2000).

[107] Tscharntke, M., Pofahl, R., Krieg, T. & Haase, I. Ras-induced spreading and wound closure in human epidermal keratinocytes. *FASEB J* **19**, 1836-1838,

(2005).

[108] Boukamp, P., Stanbridge, E. J., Foo, D. Y., Cerutti, P. A. & Fusenig, N. E. c-Ha-ras oncogene expression in immortalized human keratinocytes (HaCaT) alters growth potential in vivo but lacks correlation with malignancy. *Cancer Res* **50**, 2840-2847 (1990).

[109] Zhang, R. D., Price, J. E., Schackert, G., Itoh, K. & Fidler, I. J. Malignant potential of cells isolated from lymph node or brain metastases of melanoma patients and implications for prognosis. *Cancer Res* **51**, 2029-2035 (1991).

[110] Pastore, S. *et al.* ERK1/2 regulates epidermal chemokine expression and skin inflammation. *J Immunol* **174**, 5047-5056, (2005).

[111] Madonna, S., Scarponi, C., De Pita, O. & Albanesi, C. Suppressor of cytokine signaling 1 inhibits IFN-gamma inflammatory signaling in human keratinocytes by sustaining ERK1/2 activation. *FASEB J* **22**, 3287-3297, (2008).

[112] Moyer, J. D. *et al.* Induction of apoptosis and cell cycle arrest by CP-358,774, an inhibitor of epidermal growth factor receptor tyrosine kinase. *Cancer Res* **57**, 4838-4848 (1997).

[113] Pollack, V. A. *et al.* Inhibition of epidermal growth factor receptor-associated tyrosine phosphorylation in human carcinomas with CP-358,774: dynamics of receptor inhibition in situ and antitumor effects in athymic mice. *J Pharmacol Exp Ther* **291**, 739-748 (1999).

[114] Cappuzzo, F. *et al.* Erlotinib as maintenance treatment in advanced non-small-cell lung cancer: a multicentre, randomised, placebo-controlled phase 3 study. *Lancet Oncol* **11**, 521-529, (2010).

[115] Soto, H. *et al.* The CC chemokine 6Ckine binds the CXC chemokine receptor CXCR3. *Proc Natl Acad Sci U S A* **95**, 8205-8210 (1998).

[116] Jenh, C. H. *et al.* Cutting edge: species specificity of the CC chemokine 6Ckine signaling through the CXC chemokine receptor CXCR3: human 6Ckine is not a ligand for the human or mouse CXCR3 receptors. *J Immunol* **162**, 3765-3769 (1999).

[117] Herbst, R. S. & Langer, C. J. Epidermal growth factor receptors as a target for cancer treatment: the emerging role of IMC-C225 in the treatment of lung and head and neck cancers. *Semin Oncol* **29**, 27-36, (2002).

[118] Ethier, S. P. Signal transduction pathways: the molecular basis for targeted therapies. *Semin Radiat Oncol* **12**, 3-10, (2002).

[119] Baselga, J. Why the epidermal growth factor receptor? The rationale for cancer therapy. *Oncologist* **7 Suppl 4**, 2-8 (2002).

[120] Knobbe, C. B., Reifenberger, J. & Reifenberger, G. Mutation analysis of the Ras pathway genes NRAS, HRAS, KRAS and BRAF in glioblastomas. *Acta Neuropathol* **108**, 467-470, (2004).

[121] Meuter, S. & Moser, B. Constitutive expression of CXCL14 in healthy human and murine epithelial tissues. *Cytokine* **44**, 248-255, (2008).

[122] Hromas, R. *et al.* Cloning of BRAK, a novel divergent CXC chemokine preferentially expressed in normal versus malignant cells. *Biochem Biophys Res Commun* **255**, 703-706, (1999).

[123] Ozawa, S. *et al.* Restoration of BRAK / CXCL14 gene expression by gefitinib is associated with antitumor efficacy of the drug in head and neck squamous cell carcinoma. *Cancer Sci* **100**, 2202-2209, (2009).

[124] Kwon, J. H. *et al.* ESE-1, an enterocyte-specific Ets transcription factor, regulates MIP-3alpha gene expression in Caco-2 human colonic epithelial cells. *J Biol Chem*

278, 875-884, (2003).

[125] Miyamoto, N. G. *et al.* Interleukin-1beta induction of the chemokine RANTES promoter in the human astrocytoma line CH235 requires both constitutive and inducible transcription factors. *J Neuroimmunol* **105**, 78-90, (2000).

[126] Grove, M. & Plumb, M. C/EBP, NF-kappa B, and c-Ets family members and transcriptional regulation of the cell-specific and inducible macrophage inflammatory protein 1 alpha immediate-early gene. *Mol Cell Biol* **13**, 5276-5289 (1993).

[127] Murakami, K. *et al.* Structural and functional analysis of the promoter region of the human MCP-3 gene: transactivation of expression by novel recognition sequences adjacent to the transcription initiation site. *DNA Cell Biol* **16**, 173-183 (1997).

[128] Zhang, C., Gadue, P., Scott, E., Atchison, M. & Poncz, M. Activation of the megakaryocyte-specific gene platelet basic protein (PBP) by the Ets family factor PU.1. *J Biol Chem* **272**, 26236-26246 (1997).

[129] Minami, T., Tachibana, K., Imanishi, T. & Doi, T. Both Ets-1 and GATA-1 are essential for positive regulation of platelet factor 4 gene expression. *Eur J Biochem* **258**, 879-889 (1998).

[130] Ghadjar, P. *et al.* Chemokine receptor CCR6 expression level and liver metastases in colorectal cancer. *J Clin Oncol* **24**, 1910-1916, (2006).

[131] Rubie, C. *et al.* Enhanced expression and clinical significance of CC-chemokine MIP-3 alpha in hepatocellular carcinoma. *Scand J Immunol* **63**, 468-477, (2006).

[132] Abiko, Y. *et al.* Expression of MIP-3alpha/CCL20, a macrophage inflammatory protein in oral squamous cell carcinoma. *Arch Oral Biol* **48**, 171-175, (2003).

[133] Ghadjar, P. *et al.* Chemokine receptor CCR6 expression level and aggressiveness of prostate cancer. *J Cancer Res Clin Oncol* **134**, 1181-1189, (2008).

[134] Bordoni, R., Fine, R., Murray, D. & Richmond, A. Characterization of the role of melanoma growth stimulatory activity (MGSA) in the growth of normal melanocytes, nevocytes, and malignant melanocytes. *J Cell Biochem* **44**, 207-219, (1990).

[135] Kleeff, J. *et al.* Detection and localization of Mip-3alpha/LARC/Exodus, a macrophage proinflammatory chemokine, and its CCR6 receptor in human pancreatic cancer. *Int J Cancer* **81**, 650-657, (1999).

[136] Campbell, A. S., Albo, D., Kimsey, T. F., White, S. L. & Wang, T. N. Macrophage inflammatory protein-3alpha promotes pancreatic cancer cell invasion. *J Surg Res* **123**, 96-101, (2005).

[137] Rubie, C. *et al.* CCL20/CCR6 expression profile in pancreatic cancer. *J Transl Med* **8**, 45, (2010).

[138] Ghadjar, P., Rubie, C., Aebersold, D. M. & Keilholz, U. The chemokine CCL20 and its receptor CCR6 in human malignancy with focus on colorectal cancer. *Int J Cancer* **125**, 741-745, (2009).

[139] Rossi, D. L., Vicari, A. P., Franz-Bacon, K., McClanahan, T. K. & Zlotnik, A. Identification through bioinformatics of two new macrophage proinflammatory human chemokines: MIP-3alpha and MIP-3beta. *J Immunol* **158**, 1033-1036 (1997).

[140] Williams, I. R. CCR6 and CCL20: partners in intestinal immunity and lymphorganogenesis. *Ann N Y Acad Sci* **1072**, 52-61, (2006).

[141] Wen, H. *et al.* The chemokine receptor CCR6 is an important component of the innate immune response. *Eur J Immunol* **37**, 2487-2498, (2007).

142 Charbonnier, A. S. *et al.* Macrophage inflammatory protein 3alpha is involved in the constitutive trafficking of epidermal langerhans cells. *J Exp Med* **190**, 1755-1768 (1999).

143 Carramolino, L. *et al.* Down-regulation of the beta-chemokine receptor CCR6 in dendritic cells mediated by TNF-alpha and IL-4. *J Leukoc Biol* **66**, 837-844 (1999).

144 Page, G., Lebecque, S. & Miossec, P. Anatomic localization of immature and mature dendritic cells in an ectopic lymphoid organ: correlation with selective chemokine expression in rheumatoid synovium. *J Immunol* **168**, 5333-5341 (2002).

145 Caux, C. *et al.* Regulation of dendritic cell recruitment by chemokines. *Transplantation* **73**, S7-11 (2002).

146 Furumoto, K., Soares, L., Engleman, E. G. & Merad, M. Induction of potent antitumor immunity by in situ targeting of intratumoral DCs. *J Clin Invest* **113**, 774-783 (2004).

147 Balkwill, F., Charles, K. A. & Mantovani, A. Smoldering and polarized inflammation in the initiation and promotion of malignant disease. *Cancer Cell* **7**, 211-217, (2005).

148 Remmel, E. *et al.* Modulation of dendritic cell phenotype and mobility by tumor cells in vitro. *Hum Immunol* **62**, 39-49, (2001).

149 Lonsdorf, A. S. *et al.* Intratumor CpG-oligodeoxynucleotide injection induces protective antitumor T cell immunity. *J Immunol* **171**, 3941-3946 (2003).

150 Vollmer, J. *et al.* Characterization of three CpG oligodeoxynucleotide classes with distinct immunostimulatory activities. *Eur J Immunol* **34**, 251-262, (2004).

151 Wang, D. *et al.* CXCL1 induced by prostaglandin E2 promotes angiogenesis in colorectal cancer. *J Exp Med* **203**, 941-951, (2006).

8 Publications

8.1 Poster

September 2008

A. Hippe, **A. Schorr**, A. Müller-Homey, A. van Lierop, M. Steinhoff, S. Seeliger, R. Kubitza, E. Bünemann, R. Liersch, M. Heroult, T. K. Hoffmann, K. Jannasch, F. Alves, S. Brema, J. Sleeman, H. Augustin, A. Zlotnik, and B. Homey
"The role of the chemokine CCL20 in EGFR/Ras/ERK-mediated tumor survival, angiogenesis and progression"
Kloster Seeon 'Angiogenesis': Molecular Mechanisms and Functional Interactions, Seeon, Germany

March 2009

A. Hippe, **A. Schorr**, A. Müller-Homey, A. van Lierop, M. Steinhoff, S. Seeliger, R. Kubitza, B. Buhren, E. Bünemann, A. Gerber, R. Liersch, M. Heroult, T. K. Hoffmann, K. Jannasch, S. Brema, P. Boukamp, M. Müller, F. Alves, J. Sleeman, H. Augustin, A. Zlotnik, and B. Homey
"The role of the chemokine CCL20 in tumor-associated angiogenesis" *XXXVI. Jahrestagung der ADF, Heidelberg, Germany*

September 2009

A. Hippe, **A. Schorr**, A. Müller-Homey, A. van Lierop, M.Steinhoff, S. Seeeliger, R. Kubitza, B. Buhren, E. Bünemann, A. Gerber, R. Liersch, M. Heroult, T. K. Hoffmann, K. Jannasch, P. Boukamp, F. Alves, J. Sleeman, H. Augustin, S. A. Lira, A. Zlotnik, and B. Homey.
"EGFR/RAS/ERK-signalling-dependent production of the chemokine CCL20 in tumor cells critically contributes to angiogenesis and tumor progression"
Kloster Seeon 'The tumor-vessel interface': Cellular and molecular mechanisms of tumor progression and metastasis, Seeon, Germany

July 2010

A. Hippe, **A. Schorr**, A. Müller-Homey, S. Seeliger, K. Jannasch, B. A. Buhren, J. Sleeman, N. H. Stoecklein, F. Alves, T. K. Hoffmann, and B. Homey.

"Tumor derived CCL20 critically contributes to angiogenesis and tumor progression"
European Society for Dermatological Research 'The ESDR 2010´, Helsinki, Finland

8.2 Talks

May 2008	"Tumor-derived chemokine production generates a pro-angiogenic microenvironment" SPP1190 *Young Scientist Meeting, Würzburg*
June 2009	"Tumor derived CCL20 critically contributes to tumor angiogenesis in an EGFR/Ras – dependent manner" *Young Scientist Meeting, Düsseldorf*
May 2010	"EGFR/Ras/ERK signaling-dependent CCL20 production in tumor cells critically contributes to angiogenesis and tumor progression" *Young Investigator Meeting, Dresden*

9 Declaration

I declare that this thesis was composed by myself and that I exclusively used the indicated literature and resources. The thoughts taken directly or indirectly from external sources are properly marked as such.